Results in Physics 39 (2022) 105764

Contents lists available at ScienceDirect

Results in Physics

journal homepage: www.elsevier.com/locate/rinp

A comprehensive analysis of the stochastic fractal–fractional tuberculosis model via Mittag-Leffler kernel and white noise

Saima Rashid [a,*,1], Muhammad Kashif Iqbal [a,1], Ahmed M. Alshehri [b,1], Rehana Ashraf [c,1], Fahd Jarad [b,d,e,*,1]

[a] Department of Mathematics, Government College University, Faisalabad 38000, Pakistan
[b] Department of Mathematics, Faculty of Science, King Abdulaziz University, P.O. Box 80203, Jaddeh 21589, Saudi Arabia
[c] Department of Mathematics, Lahores College for Women University, Lahore, Pakistan
[d] Department of Mathematics, Cankaya University, Ankara, Turkey
[e] Department of Medical Research, China Medical University Hospital, China Medical University, Taichung, Taiwan

ARTICLE INFO

MSC:
26A51
26A33
26D07
26D10
26D15

Keywords:
Tuberculosis model
Fractal–fractal differential operators
Stochastic modelling
Qualitative analysis
Numerical solutions

ABSTRACT

In this research, we develop a stochastic framework for analysing tuberculosis (TB) evolution that includes newborn immunization via the fractal–fractional (F–F) derivative in the Atangana–Baleanu sense. The population is divided into four groups by this system: susceptibility $\mathbf{S}(\xi)$, infectious $\mathbf{I}(\xi)$, immunized infants $\mathbf{V}(\xi)$, and restored $\mathbf{R}(\xi)$. The stochastic technique is used to describe and assess the invariant region, basic reproduction number, and local stability for disease-free equilibrium. This strategy has significant modelling difficulties since it ignores the unpredictability of the system phenomena. To prevent such problems, we convert the deterministic strategy to a randomized one, which seems recognized to have a vital influence by adding an element of authenticity and fractional approach. Owing to the model intricacies, we established the existence-uniqueness of the model and the extinction of infection was carried out. We conducted a number of experimental tests using the F–F derivative approach and obtained some intriguing modelling findings in terms of (i) varying fractional-order (φ) and fixing fractal-dimension (ω), (ii) varying ω and fixing φ, and (iii) varying both φ and ω, indicating that a combination of such a scheme can enhance infant vaccination and adequate intervention of infectious patients can give a significant boost.

Introduction

Tuberculosis (TB) is a viral infection caused by mycobacterium that is spread through the air when people with active TB (chronologically TB) breathe, inhale, converse, or shout [1,2]. It mostly affects the lungs, and it can impact the endocrine circulation, circulatory vessels, cranium, spinal cord, and renal, influenza, calorie restriction, breathlessness, coughing uncontrollably, feeling fatigued all the time, nocturnal sickness, lack of energy, and starvation are all indications of chronic TB, (see, Fig. 1–Fig. 2). Bacterial infections are prevalent nowadays. In impoverished areas, tuberculosis is a significant global healthcare risk [3]. It impacts people of all ages and from all walks of life. However, the current figures for 2018 show that 89 percent of incidents were grownups (57 percent men, 32 percent older females) and 11 percent were kids. Furthermore, 8.6 percent of the population was HIV-positive (compared to 72 percent in Africa) [4]. In 2018, the WHO zones of Asian countries (44 percent), Africa (24 percent), and Southern Asia (18 percent) had the highest proportion of Tb patients, followed by the Eastern Gulf (8 percent), the Caribbean (3 percent), and Europeans (3 percent). Furthermore, Pakistan (27 percent), Russia (9 percent), the Netherlands (8 percent), Korea (6 percent), Argentina (6 percent), Ethiopia (4 percent), Albania (4 percent), and Namibia (4 percent each) contributed three-quarters of total production. These states, along with 22 others in WHO's classification of 30 areas with strong TB burdens, represented 87 percent of global occurrences [5].

This is probably one of Ethiopia's least significant environmental safety problems, harming about 30,000 individuals every year [6]. According to the World Health Organization, Africa is the third most tuberculosis-affected African country and the eighth most tuberculosis-affected nation on the planet [7], accounting for 80 percent of tuberculosis infection globally. Youthful individuals are frequently affected:

* Corresponding author.
E-mail addresses: saimarashid@gcuf.edu.pk (S. Rashid), kashifiqbal@gcuf.edu.pk (M.K. Iqbal), amalshehre@kau.edu.sa (A.M. Alshehri), rehanaashraf467@gmail.com (R. Ashraf), fahd@cankaya.edu.tr (F. Jarad).
[1] All authors contributed equally.

https://doi.org/10.1016/j.rinp.2022.105764
Received 19 June 2022; Received in revised form 22 June 2022; Accepted 24 June 2022
Available online 28 June 2022

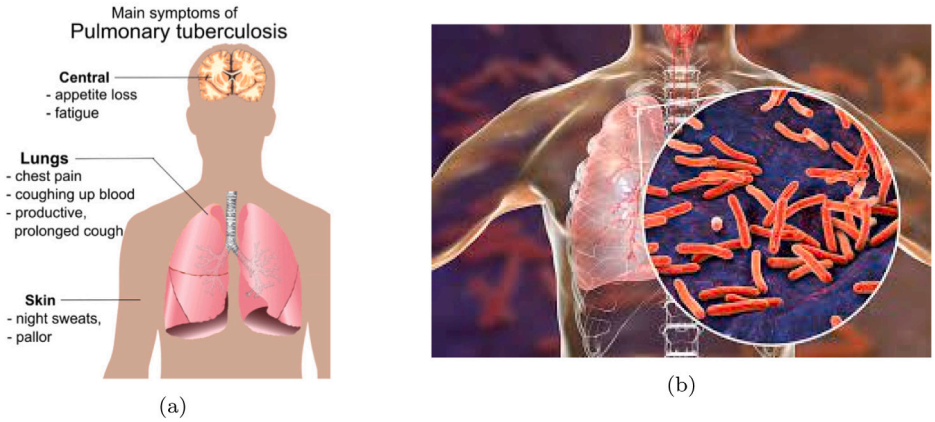

Fig. 1. Tuberculosis symptoms and their effects on the human body.

58 percent of all reported diagnoses in Pakistan are under 35 years old, and 39 percent of the projected 32,000 fatalities annually were among those aged 15 to 64, which led to the demise of household income producers and caregivers of young children. This places a new internal and external responsibility on Pakistan's youth, who are the country's present and prospective financial foundation [8].

People can avoid contracting tuberculosis by following appropriate therapeutic guidelines, such as accepting all practitioner medications for the specified time-frame, adhering to all schedules, invariably protecting the throat with a parenchyma when breathing normally, assigning used paper tissues in a trash container and putting them aside, not being allowed to meet other humans and not encouraging them to meet up, returning to the office, university, etc. Another preventive measure is immunization [9]. Bacillus Calmette Guerin (BCG) inoculation is administered to prevent tuberculosis. BCG vaccination was included in the immunization schedule in 1973 [10]. The effectiveness of BCG in controlling respiratory infections in individuals is hugely diverse [11]. The BCG immunization of infants diminishes the prevalence of tuberculosis by more than half in general [12]. The term "neonates born" generally refers to a baby who is between the ages of infancy and twelve weeks [13].

Numerical modelling has been demonstrated to be an effective technique for analysing the transmission and prevention of communicable infections, as well as for setting priorities for effective interventions for vaccination programmes [13]. Identifying the patterns of virus propagation in individuals, states, and continents can contribute to improving measures to reduce communicable illness [9]. For further information on TB, we refer the interested readers [14–18].

Recently, the investigation of Lévy motion, continuous random walk, and banking data contributed to the development of fractional calculus, which has a broad array of implementations in chemical reactions, thermodynamics, mechanics, quantum dynamics, remote sensing and systems identification, cognitive science, photon logistics, rheology, data analysis, and other disciplines [19–21]. Both fractional derivative/integral operators have been acknowledged as effective computational instruments capable of acquiring inhomogeneities that the classical differential and integral operators are incapable of capturing. Furthermore, it is worth noting that fractal–fractional operators record various sorts of heterogeneities and perform differently when modelling biological and scientific phenomena. We can understand that there are certainly numerous practical challenges that neither fractional nor fractal formulations can adequately recreate on an individualized level. As a result, scientists concluded that they were in desperate need of innovative mathematical operators to simulate such complex structures. Although some views hold that there is nothing new or revolutionary, it is hard to conclude that integrating two current ideas can lead to a revolutionary mechanism. A novel differential operator was initially enacted in [22] to incorporate greater intricacies. The combination of the fractal differentiation of a fractional derivative of a particular mapping could be interpreted as this scientific expression. Obviously, it depends on the kernel, three interpretations were proposed. The concept was challenged and applied to a variety of problems, including chaotic attractors, epidemics, and dispersion, among others [23–25], and the majority of the articles included produced some excellent simulated predictions.

Historically, solutions of ordinary differential equations (DE) and partial differential equations (PDE) have long been used to create numerical simulations for complex interactions in pharmacological, biomedical, electrical, and scientific methods. The prevalence and exclusivity of numerical solution approaches serve as the foundation for accuracy assessment and subsequent investigation of the relevant nonlinear phenomena. The research has also broadened to frameworks of temporal delay/functional nonlinear problems [26], which include the inherited feature of complex interactions in fields of science and engineering. For obvious computational purposes, the mechanisms of ordinary Itô–Doob type stochastic DEs [27], stochastic PDEs [28], stochastic fractional DEs [29], and stochastic fractional PDEs in abstract environments [30] were characterized in the foundation of Itô–Doob type stochastic integral equations around 1960. The normalization Wiener procedure [31] describes the consequences of stochastic environmental perturbations. This was developed extensively using local martingale integrals [32]. We perceive that scientists increasingly pursue improvements of essential component notions that consume the understanding of initial guess to its corresponding integral equation concern, predicated on the aforesaid contextualized creation of interactive modelling and to implement additional functional and/or randomized disturbance attributes of interaction into the mathematical analysis outlined by DEs.

Recently, stochastic vibrant frameworks for financial documents (capitalization) were developed using a combination of conventional numerical techniques and stochastic approaches in [33]. We require to update the emerging mathematical formulas by consciously implementing specific considerable directly attributed specifications or characteristics with system parameters in attempt to enhance this framework to more massively intricate mechanisms in physical sciences functioning under intrinsic functional and outer randomized interference. In 2021, Atangana and Araz [34] introduced a revolutionary idea of modelling and forecasting the spread of COVID-19 with stochastic and deterministic approaches in Africa and Europe. Alkahtani and Koca [35] presented the fractional stochastic SIR model via the fractional calculus approach and Alkahtani and Alzaid [36] contemplated the stochastic mathematical model of chikungunya spread with the global derivative.

Simulation is required for contagious TB for a myriad of reasons, including the reality that TB has an intricate and incompletely comprehended evolutionary legacy, the difficulty of performing endovascular

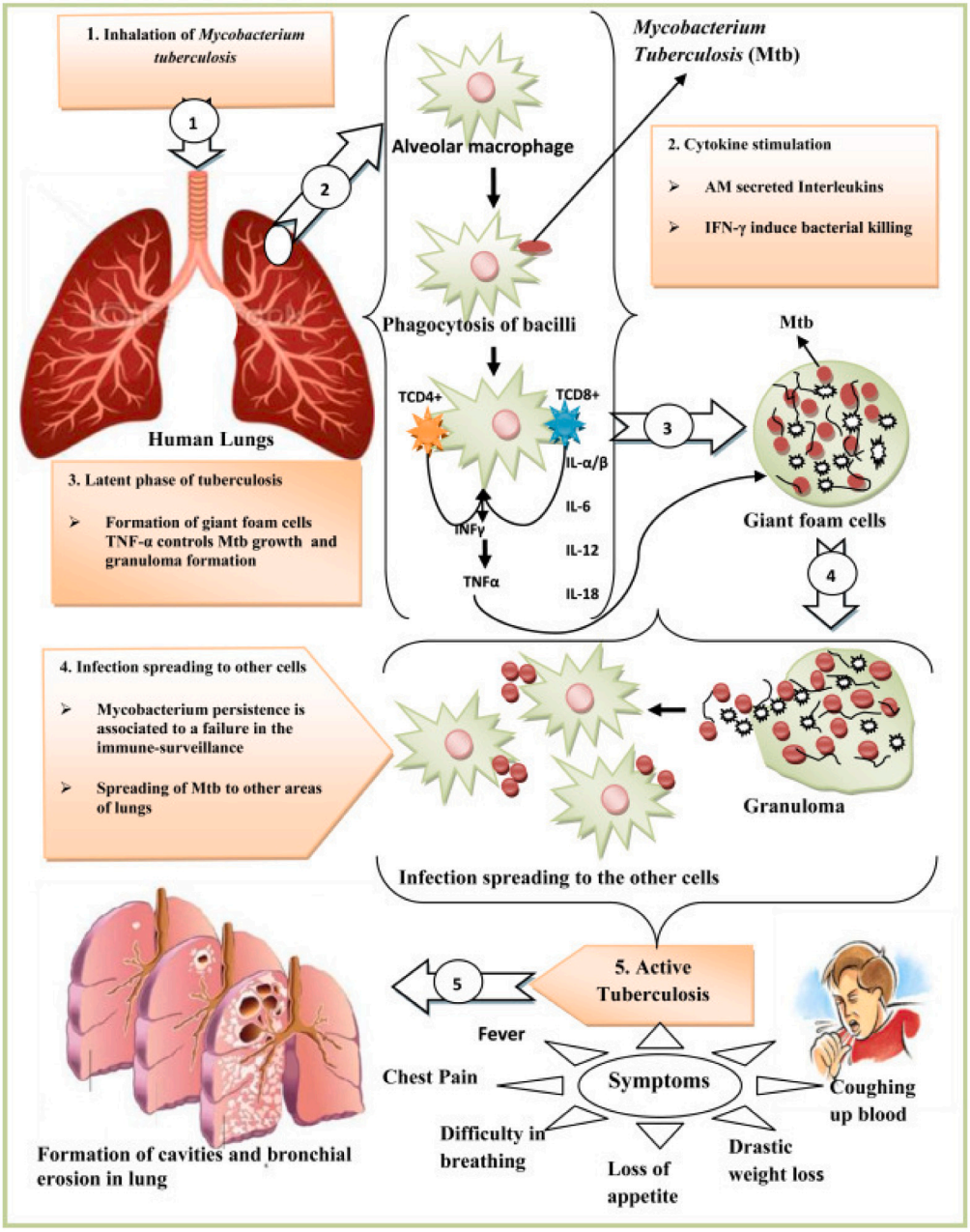

Fig. 2. Initial colonization process of tuberculosis disease.

investigations due to the latency between infestation and illness, the necessity to better understand the behaviour of the especially vulnerable community, fiscal problems in performing therapies in underdeveloped and developed regions, and numerous lingering inquiries about the implications of inter-country transmission. Because M. tuberculosis spread and TB diagnosis are impacted by a lot of complicated biochemical pathways, the occurrence of unpredictability in the vaccine's spreading characteristics could be assumed [37]. Taking most of these aspects into account, a stochastic simulation of tuberculosis is now widely used, with the characteristics perturbed.

In this paper, a new mechanism termed fractal–fractional is implemented to construct an SVIRS stochastic system for TB transmission that takes infant immunization into account. For clarity purposes, Atangana–Baleanu derivative concept is taken into consideration with the Browning motion. We designed a TB system and validated its properties using authentic propagation scenarios utilizing the F–F technique. We apply F–F pattering to real-life data from TB patients and discover a slew of surprising results when newborns have been vaccinated. Eventually, we present a detailed description of the F–F operator, which is subsequently adhered to our suggested framework with fascinating numerical findings with varying fractal-dimension and fractional-order. We have shown that when $\mathbb{R}_0^S < 1$ then the infection wipes out. Also, we computed that if $\mathbb{R}_0^S > 1$, then there will be a persistence of disease in the population. Existence-uniqueness analysis is also demonstrated with the Lipschitiz conditions and linear growth requirements. Furthermore, the extinction of disease has developed. Finally, the investigation is encapsulated; (for parameter descriptions, see, Table 1).

Preliminaries

It is vital to investigate some basic F–F operator theories before continuing on to the mathematical formulation. Consider the function $\mathbf{y}(\xi)$, which is continuous and fractal differentiable on $[c, d]$ with

Table 1
Parameter's specifications.

Parameters	Data estimated	References
π	2.8	[6]
δ_1	0.0453	[15]
δ_2	0.04	[16]
ϑ	0.07	[17]
ρ_2	0.1	[12]
ζ	0.2	[10]
$\mathbf{q}$	0.5	[37]
γ	0.01	[18]
ρ_1	0.4	[12]
χ	0.1	[17]

fractal-dimension ω and fractional-order φ, as well as the specifications available in [22].

Definition 1 ([22]). The F-FO of $\mathbf{y}(\xi)$ containing the PL kernel in the context of Riemann–Liouville (RL) can be stated as follows for $\varphi \in [0,1]$:

$$^{FFP}\mathbf{D}^{\varphi,\omega}_{0,\xi}(\mathbf{y}(\xi)) = \frac{1}{\Gamma(\mathbf{u}-\varphi)}\frac{d}{d\xi^{\omega}}\int_0^{\xi}(\xi-\mathbf{x})^{\mathbf{u}-\varphi-1}\mathbf{y}(\mathbf{x})d\mathbf{x}, \tag{1}$$

where $\frac{d\mathbf{y}(\mathbf{x})}{d\mathbf{x}^{\omega}} = \lim_{\xi\mapsto\mathbf{x}}\frac{\mathbf{y}(\xi)-\mathbf{y}(\mathbf{x})}{\xi^{\omega}-\mathbf{x}^{\omega}}$ and $\mathbf{u}-1<\varphi,\omega\le\mathbf{u}\in\mathbb{N}$.

Definition 2 ([22]). The F-FO of $\mathbf{y}(\xi)$ containing the ED kernel in the context of RL can be stated as follows for $\varphi\in[0,1]$:

$$^{FFE}\mathbf{D}^{\varphi,\omega}_{0,\xi}(\mathbf{y}(\xi)) = \frac{\mathbb{M}(\varphi)}{1-\varphi}\frac{d}{d\xi^{\omega}}\int_0^{\xi}\exp\Big(-\frac{\varphi}{1-\varphi}(\xi-\mathbf{x})\Big)\mathbf{y}(\mathbf{x})d\mathbf{x}, \tag{2}$$

such that $\mathbb{M}(0)=\mathbb{M}(1)=1$ having $\varphi>0,\ \omega\le\mathbf{u}\in\mathbb{N}$.

Definition 3 ([21]). The F-FO of $\mathbf{y}(\xi)$ containing the GML kernel in the context of Riemann–Liouville (RL) can be stated as follows for $\varphi\in[0,1]$:

$$^{FFM}\mathbf{D}^{\varphi,\omega}_{0,\xi}(\mathbf{y}(\xi)) = \frac{\mathbb{ABC}(\varphi)}{1-\varphi}\frac{d}{d\xi^{\omega}}\int_0^{\xi}E_{\varphi}\Big(-\frac{\varphi}{1-\varphi}(\xi-\mathbf{x})\Big)\mathbf{y}(\mathbf{x})d\mathbf{x}, \tag{3}$$

such that $\mathbb{ABC}(\varphi)=1-\varphi+\frac{\varphi}{\Gamma(\varphi)}$ having $\varphi>0,\ \omega\le1\in\mathbb{N}$.

Definition 4 ([22]). The corresponding F–F integral formulation of (1) is defined as:

$$^{FFP}\mathbb{J}^{\varphi}_{0,\xi}(\mathbf{y}(\xi)) = \frac{\omega}{\Gamma(\varphi)}\int_0^{\xi}(\xi-\mathbf{x})^{\varphi-1}\mathbf{x}^{\omega-1}\mathbf{y}(\mathbf{x})d\mathbf{x}. \tag{4}$$

Definition 5 ([22]). The corresponding F–F integral formulation of (2) is defined as:

$$^{FFE}\mathbb{J}^{\varphi}_{0,\xi}(\mathbf{y}(\xi)) = \frac{\varphi\omega}{\mathbb{M}(\varphi)}\int_0^{\xi}\mathbf{x}^{\omega-1}\mathbf{y}(\mathbf{x})d\mathbf{x}+\frac{\omega(1-\varphi)\xi^{\omega-1}\mathbf{y}(\xi)}{\mathbb{M}(\varphi)}. \tag{5}$$

Definition 6 ([22]). The corresponding F–F integral formulation of (3) is defined as:

$$^{FFM}\mathbb{J}^{\varphi}_{0,\xi}(\mathbf{y}(\xi)) = \frac{\varphi\omega}{\mathbb{ABC}(\varphi)}\int_0^{\xi}\mathbf{x}^{\omega-1}(\xi-\mathbf{x})^{\varphi-1}\mathbf{y}(\mathbf{x})d\mathbf{x}+\frac{\omega(1-\varphi)\xi^{\omega-1}\mathbf{y}(\xi)}{\mathbb{ABC}(\varphi)}. \tag{6}$$

Definition 7 ([21]). Let $\mathbf{y}\in H^1(\mathbf{c},\mathbf{d})$, $\mathbf{c}<\mathbf{d}$ and the Atangana–Baleanu fractional derivative operator is defined as:

$$^{ABC}_{\mathbf{c}}\mathbf{D}^{\varphi}_{\xi}(\mathbf{y}(\xi)) = \frac{\mathbb{ABC}(\varphi)}{1-\varphi}\int_{\mathbf{c}}^{\xi}\mathbf{y}'(\mathbf{x})E_{\varphi}\Big(-\frac{\varphi(\xi-\mathbf{x})^{\varphi}}{1-\varphi}\Big)d\mathbf{x},\quad \varphi\in[0,1], \tag{7}$$

where $\mathbb{ABC}(\varphi)$ denotes the normalization function.

Definition 8 ([38]). The Gaussian hypergeometric function $_2\mathcal{F}_1$, described by

$$_2\mathcal{F}_1(y_1,y_2;y_3,y_4) = \frac{1}{\mathbb{B}(y_2,y_3-y_2)}\int_1^{1}\xi^{y_2-1}(1-\xi)^{y_3-y_2-1}(1-y_4\xi)^{-y_1}d\xi,\quad (y_3>y_2>0,|y_1|<1), \tag{8}$$

where $\mathbb{B}(y_1,y_2)=\frac{\Gamma(y_1)\Gamma(y_2)}{\Gamma(y_1+y_2)}$ and $\Gamma(y_1)=\int_0^{\infty}\exp(-\xi)\xi^{y_1}d\xi$ is the Gamma function.

Conception and illustration of the model

The proposed framework divides the overall population into four cohorts or categories based on clinical characteristics: susceptibility $\mathbf{S}(\xi)$, infectious $\mathbf{I}(\xi)$, immunized $\mathbf{V}(\xi)$, and restored $\mathbf{R}(\xi)$, respectively.

People of all generations who have not had productive interactions with the streptococcus are included in the susceptibility group, $\mathbf{S}(\xi)$. Persons of all categories diagnosed with tuberculosis in the process of formation belong to the infectious group, $\mathbf{I}(\xi)$; from the diseased category, a person receives therapy and moves to the restored group, $\mathbf{R}(\xi)$. People who were inoculated as neonates and only have a moderate susceptibility to tuberculosis (TB) are classified as inoculated, $\mathbf{V}(\xi)$. Considering the enlistment π of probability lies somewhere between 0 and 1, the inoculated category is augmented through birth. Birth increases the recruitment yield of the highly vulnerable group to π of possibility $1-\mathbf{q}$, as well as from the immunocompetent category $\mathbf{V}$ at a rate of $b1(b1\ge0)$ and from the retrieved group $\mathbf{R}$ at a rate of χ.

In this scenario, δ_1 represents the spontaneous mortality rate, δ_2 represents the illness fatality proportion for people in cohort $\mathbf{I}$, and ϑ represents the probability that one contaminated person per interaction per unit of time infects susceptibility $\mathbf{S}$ and immunized $\mathbf{V}$ people. Then there is $\vartheta\rho_2$, and that is the proportion where such susceptibility people become infectious, and $\gamma\vartheta\rho_2$, which is the proportion at which immunized people become contaminated. If $\gamma=0$, inoculation prevention effectiveness is 100 percent; if $\gamma=1$, vaccination protective efficacy is 0; and $1-\gamma$ indicates a decrease in contamination risk due to inoculation performance. ζ refers to the rate at which an affected person exits the infection cohort ($\mathbf{I}$) and enters the group ($\mathbf{R}$). The propagation system is predicated on the SVIRS concept. $\mathbf{N}(\xi)$ represents the overall population at time ξ, and thus $\mathbf{N}(\xi)=\mathbf{S}(\xi)+\mathbf{V}(\xi)+\mathbf{I}(\xi)+\mathbf{R}(\xi)$.

We surmise that there is a cohesive group of people in the community. That indicates that each un-immunized person has a fair probability of becoming contaminated when they come into contact with a potentially infected person and that pathogen propagation appears at a regular prevalence speed. Furthermore, we expect certain applicants to emerge at a rate of $1-\mathbf{q}$ in the highly vulnerable class $\mathbf{S}$ and at a rate of $\mathbf{q}$ in the inoculated class $\mathbf{V}$. Because the BCG medication's usefulness is not perfect, several immunized people will become infectious with microbes. Because the inoculated presenter's protection is decreasing, certain immunized people will be exposed to pathogens exhibiting an incidence ρ_1. We suppose that restored people migrate to the vulnerable group at a pace of χ resulting in a loss of immunization. We also presume that all of the system's characteristics are non-negative.

The fundamental complexities of tuberculosis to newborn inoculation are depicted in Fig. 3 as a process flow, taking into account the concepts, suppositions, and inter-dependencies between the factors and specifications. The model is presented as

$$\begin{cases}\frac{d\mathbf{S}(\xi)}{d\xi} = (1-\mathbf{q})\pi+\rho_1\mathbf{V}+\chi\mathbf{R}-\delta_1\mathbf{S}-\vartheta\rho_2\mathbf{SI},\\ \frac{d\mathbf{V}(\xi)}{d\xi} = \mathbf{q}\pi-\gamma\rho_2\vartheta\mathbf{VI}-(\rho_1+\delta_1)\mathbf{V},\\ \frac{d\mathbf{I}(\xi)}{d\xi} = \vartheta\varsigma\mathbf{SI}+\gamma\vartheta\rho_2\mathbf{VI}-(\delta_1+\delta_2+\zeta)\mathbf{I},\\ \frac{d\mathbf{R}(\xi)}{d\xi} = \zeta\mathbf{I}-\chi\mathbf{R}-\delta_1\mathbf{R},\end{cases} \tag{9}$$

subject to ICs $\mathbf{S}(0)=\mathbf{S}_0\ge0$, $\mathbf{V}(0)=\mathbf{V}_0\ge0$, $\mathbf{I}(0)=\mathbf{I}_0\ge0$, $\mathbf{R}(0)=\mathbf{R}_0\ge0$.

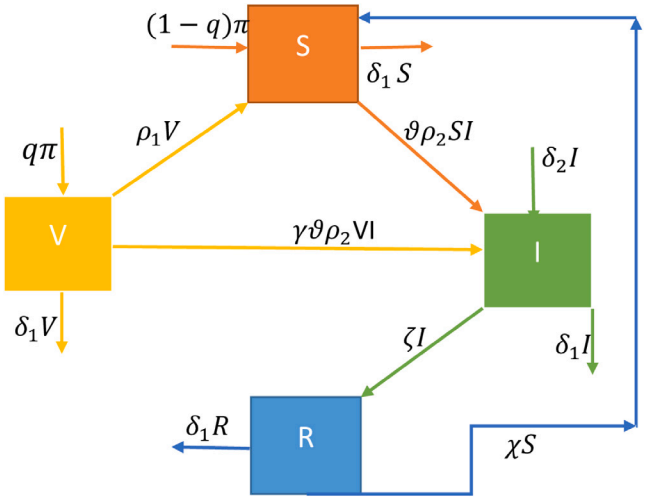

Fig. 3. Flow chart for tuberculosis model.

Even though physiological mechanisms implicated in the complexities of tuberculosis are stochastic instead of prescriptive, ignoring their constructed unpredictability might indeed result in misrepresentative and inaccurate outcomes [37]. The classification algorithm seems to have some restrictions in numerical simulations of virus propagation. Stochastic DES systems exert an important influence in a variety of fields because they offer a higher sense of authenticity than their predictable equivalents. Several writers have successfully investigated the behaviour of modelling techniques that include variable modification. As a result, to account for the influence of sporadic dynamic capabilities, we include white noise in every component of the framework in this work. Assume that a probabilistic environmental condition affects every single person in the community at the same time. The completely exclusive ordinary Brownian motions with $B_j(0) = 0$ are denoted by $B_j(\xi)$ and σ_j, $j = 1, 2, 3, 4$, the white noise sensitivities. The stochastic analogue of the deterministic framework (9) assumes the appropriate structure when stochastic disturbance is introduced:

$$\begin{cases} d\mathbf{S}(\xi) = \big((1-\mathbf{q})\pi + \rho_1\mathbf{V} + \chi\mathbf{R} - \delta_1\mathbf{S} - \vartheta\rho_2\mathbf{SI}\big)d\xi + \sigma_1\mathbf{S}B_1(\xi), \\ d\mathbf{V}(\xi) = \big(\mathbf{q}\pi - \gamma\rho_2\vartheta\mathbf{VI} - (\rho_1+\delta_1)\mathbf{V}\big)d\xi + \sigma_2\mathbf{V}B_2(\xi), \\ d\mathbf{I}(\xi) = \big(\vartheta\varsigma\mathbf{SI} + \gamma\vartheta\rho_2\mathbf{VI} - (\delta_1+\delta_2+\zeta)\mathbf{I}\big)d\xi + \sigma_3\mathbf{I}B_3(\xi), \\ d\mathbf{R}(\xi) = \big(\zeta\mathbf{I} - \chi\mathbf{R} - \delta_1\mathbf{R}\big)d\xi + \sigma_4\mathbf{R}B_4(\xi). \end{cases} \tag{10}$$

Qualitative analysis

Invariant region

To find the invariant region for (10), we surmise the over population $\mathbf{N}(\xi) = \mathbf{S}(\xi) + \mathbf{V}(\xi) + \mathbf{I}(\xi) + \mathbf{R}(\xi)$.

Theorem 1. *Suppose there be a domain* $\Lambda = \big\{(\mathbf{S},\mathbf{V},\mathbf{I},\mathbf{R}) \in \mathbb{R}^4_+ : 0 \le \mathbf{N}(\xi) \le \pi/\delta_1\big\}$ *at which the stochastic system equation's* (10) *is almost probably positive invariant.*

Proof. Suppose $\mathcal{K}_0$ supposed to be the largest integer. Therefore, if $(\mathbf{S}_0,\mathbf{V}_0,\mathbf{I}_0,\mathbf{R}_0) \in \mathbb{R}^4_+$, then each factor of $(\mathbf{S}_0,\mathbf{V}_0,\mathbf{I}_0,\mathbf{R}_0)$ stays in $\left[\frac{1}{\mathbb{k}_0}, 1\right]$ For every integer $\mathcal{K} \ge \mathbb{k}_0$ Stopping time can be defined as follows:

$$\begin{aligned} \Omega_{\mathbb{k}} &= \inf\Big\{\xi \in [0,\Omega_\epsilon] : \mathbf{S}(\xi) \le \frac{1}{\mathbb{k}},\ or\mathbf{I}(\xi) \le \frac{1}{\mathbb{k}},\ \mathbf{R}(\xi) \le \frac{1}{\mathbb{k}}\Big\}, \\ \Omega_{\infty} &= \inf\Big\{\xi \in [0,\Omega_\epsilon] : \mathbf{S}(\xi) \le 0,\ or\mathbf{I}(\xi) \le 0,\ \mathbf{R}(\xi) \le 0\Big\}. \end{aligned} \tag{11}$$

Our aim is to illustrate that $\mathbf{P}(\Omega = \infty)$, i.e., $\mathbf{P}(\Omega < \Psi)$, $for\ \Psi > 0$, so that we can demonstrate $\lim_{\xi\mapsto\infty}\sup\mathbf{P}(\Omega_{\mathbb{k}} < 0) = 0$.

Define a Lyapunov functional $\mathcal{V}$ as

$$\mathcal{V}(\xi) = \ln\frac{1}{\mathbf{S}(\xi)} + \ln\frac{1}{\mathbf{V}(\xi)} + \ln\frac{1}{\mathbf{I}(\xi)} + \ln\frac{1}{\mathbf{R}(\xi)}.$$

In view of Itô's approach, for $\Psi > 0$, $\xi \in [0, \Psi \wedge \Omega_{\mathbb{k}}]$ to $\mathbf{Y}(\xi) = \big(\mathbf{S}(\xi),\mathbf{V}(\xi),\mathbf{I}(\xi),\mathbf{R}(\xi)\big)$, we find

$$\begin{aligned} d\mathcal{V}(\xi) = -\Big(&\frac{1}{\mathbf{S}(\xi)}d\mathbf{S}(\xi) + \frac{1}{\mathbf{V}(\xi)}d\mathbf{V}(\xi) + \frac{1}{\mathbf{I}(\xi)}d\mathbf{I}(\xi) + \frac{1}{\mathbf{R}(\xi)}d\mathbf{R}(\xi) \\ &- \frac{1}{\mathbf{S}^2(\xi)}d\mathbf{S}^2(\xi) - \frac{1}{\mathbf{I}^2(\xi)}d\mathbf{I}^2(\xi)\Big). \end{aligned}$$

Thus, we have

$$\begin{aligned} d\mathcal{V}(\xi) =& -\frac{1}{\mathbf{S}(\xi)}\Big\{\big((1-\mathbf{q})\pi + \rho_1\mathbf{V} + \chi\mathbf{R} - \delta_1\mathbf{S} - \vartheta\rho_2\mathbf{SI}\big)d\xi + \sigma_1\mathbf{S}B_1(\xi)\Big\} \\ &-\frac{1}{\mathbf{I}(\xi)}\Big\{\big(\vartheta\varsigma\mathbf{SI} + \gamma\vartheta\rho_2\mathbf{VI} - (\delta_1+\delta_2+\zeta)\mathbf{I}\big)d\xi + \sigma_3\mathbf{I}B_3(\xi)\Big\} \\ &-\frac{1}{\mathbf{V}(\xi)}\Big\{\big(\mathbf{q}\pi - \gamma\rho_2\vartheta\mathbf{VI} - (\rho_1+\delta_1)\mathbf{V}\big)d\xi + \sigma_2\mathbf{V}B_2(\xi)\Big\} \end{aligned} \tag{12}$$

$$\begin{aligned} &-\frac{1}{\mathbf{R}(\xi)}\Big\{\big(\zeta\mathbf{I} - \chi\mathbf{R} - \delta_1\mathbf{R}\big)d\xi + \sigma_4\mathbf{R}B_4(\xi)\Big\} \\ &-\frac{1}{\mathbf{S}^2(\xi)}\Big\{\big((1-\mathbf{q})\pi + \rho_1\mathbf{V} + \chi\mathbf{R} - \delta_1\mathbf{S} - \vartheta\rho_2\mathbf{SI}\big)d\xi + \sigma_1\mathbf{S}B_1(\xi)\Big\}^2 \\ &+\frac{1}{\mathbf{I}^2(\xi)}\Big\{\big(\vartheta\varsigma\mathbf{SI} + \gamma\vartheta\rho_2\mathbf{VI} - (\delta_1+\delta_2+\zeta)\mathbf{I}\big)d\xi + \sigma_3\mathbf{I}B_3(\xi)\Big\}^2. \end{aligned} \tag{13}$$

Setting $\mathcal{A}_1 = (1-\mathbf{q})\pi + \rho_1\mathbf{V} + \chi\mathbf{R} - \delta_1\mathbf{S} - \vartheta\rho_2\mathbf{SI}$, $\mathcal{A}_2 = \sigma_1\mathbf{S}(\xi)$, $\mathcal{A}_3 = \vartheta\varsigma\mathbf{SI} + \gamma\vartheta\rho_2\mathbf{VI} - (\delta_1+\delta_2+\zeta)\mathbf{I}$ and $\mathcal{A}_4 = \sigma_2\mathbf{I}(\xi)$, then (12) reduces to

$$\begin{aligned} d\mathcal{V}(\xi) =& -\frac{1}{\mathbf{S}(\xi)}\Big\{\big((1-\mathbf{q})\pi + \rho_1\mathbf{V} + \chi\mathbf{R} - \delta_1\mathbf{S} - \vartheta\rho_2\mathbf{SI}\big)d\xi + \sigma_1\mathbf{S}B_1(\xi)\Big\} \\ &-\frac{1}{\mathbf{I}(\xi)}\Big\{\big(\vartheta\varsigma\mathbf{SI} + \gamma\vartheta\rho_2\mathbf{VI} - (\delta_1+\delta_2+\zeta)\mathbf{I}\big)d\xi + \sigma_3\mathbf{I}B_3(\xi)\Big\} \\ &-\frac{1}{\mathbf{V}(\xi)}\Big\{\big(\mathbf{q}\pi - \gamma\rho_2\vartheta\mathbf{VI} - (\rho_1+\delta_1)\mathbf{V}\big)d\xi + \sigma_2\mathbf{V}B_2(\xi)\Big\} \\ &-\frac{1}{\mathbf{R}(\xi)}\Big\{\big(\zeta\mathbf{I} - \chi\mathbf{R} - \delta_1\mathbf{R}\big)d\xi + \sigma_4\mathbf{R}B_4(\xi)\Big\} \\ &-\frac{1}{\mathbf{S}^2(\xi)}\Big\{\mathcal{A}_1^2d^2\xi + \mathcal{A}_1\mathcal{A}_2d\xi dB_1(\xi) + \mathcal{A}_2^2d^2B_1(\xi)\Big\} \\ &+\frac{1}{\mathbf{I}^2(\xi)}\Big\{\mathcal{A}_3^2d^2\xi + \mathcal{A}_3\mathcal{A}_4d\xi dB_3(\xi) + \mathcal{A}_4d^2B_3(\xi)\Big\}. \end{aligned}$$

It follows that

$$\begin{aligned} d\mathcal{V}(\xi) =& -\Big\{\Big(\frac{(1-\mathbf{q})\pi}{\mathbf{S}(\xi)} + \frac{\rho_1\mathbf{V}(\xi)}{\mathbf{S}(\xi)} + \frac{\chi\mathbf{R}(\xi)}{\mathbf{S}(\xi)} - \delta_1 - \vartheta\rho_2\mathbf{I}(\xi)\Big)d\xi + \sigma_1dB_1(\xi)\Big\} \\ &-\Big\{\big(\vartheta\rho_2\mathbf{S}(\xi) + \gamma\vartheta\rho_2\mathbf{V}(\xi) - (\delta_1+\delta_2+\zeta)\big) + \sigma_3B_3(\xi)\Big\} \\ &-\Big\{\Big(\frac{\mathbf{q}\pi}{\mathbf{V}(\xi)} - \gamma\rho_2\vartheta\mathbf{I}(\xi) - (\rho_1+\delta_1)\Big) + \sigma_2dB_2(\xi)\Big\} \\ &-\Big\{\Big(\frac{\zeta\mathbf{I}(\xi)}{\mathbf{R}(\xi)} - (\chi+\delta_1)\Big)d\xi + \sigma_4dB_4(\xi)\Big\} \\ &-\Big\{\sigma_1^2 + \sigma_2^2 + \sigma_3^2 + \sigma_4^2\Big\}d\xi \\ &-\Big\{\sigma_1dB_1(\xi) + \sigma_2dB_2(\xi) + \sigma_3dB_3(\xi) + \sigma_4dB_4(\xi)\Big\}. \end{aligned}$$

After simplification, the aforesaid equation reduced to

$$d\mathcal{V}(\xi) = \mathcal{H}\mathcal{V}d\xi - \Big\{\sigma_1dB_1(\xi) + \sigma_2dB_2(\xi) + \sigma_3dB_3(\xi) + \sigma_4dB_4(\xi)\Big\},$$

where $\mathcal{H}\mathcal{V} = -\frac{(1-\mathbf{q})\pi}{\mathbf{S}(\xi)} - \frac{\rho_1\mathbf{V}(\xi)}{\mathbf{S}(\xi)} - \frac{\chi\mathbf{R}(\xi)}{\mathbf{S}(\xi)} + \delta_1 + \vartheta\rho_2\mathbf{I}(\xi) - \vartheta\rho_2\mathbf{S}(\xi) - \gamma\vartheta\rho_2\mathbf{V}(\xi) + (\delta_1+\delta_2+\zeta) - \frac{\mathbf{q}\pi}{\mathbf{V}(\xi)} + \gamma\rho_2\vartheta\mathbf{I}(\xi) + (\rho_1+\delta_1) - \frac{\zeta\mathbf{I}(\xi)}{\mathbf{R}(\xi)} + (\chi+\delta_1) + \sigma_1^2 + \sigma_2^2 + \sigma_3^2 + \sigma_4^2 = C.$

Thus, we have

$$d\mathcal{V}(\xi) \le Cd\xi - \Big\{\sigma_1dB_1(\xi) + \sigma_2dB_2(\xi) + \sigma_3dB_3(\xi) + \sigma_4dB_4(\xi)\Big\}.$$

Performing integration from 0 *to* $\Omega_{\mathbb{k}\wedge\Psi}$, it can be deduced that

$$\begin{aligned} \int_0^{\Omega_{\mathbb{k}\wedge\Psi}} d\mathcal{V}(\mathbf{Y}(\xi)) \le& \int_0^{\Omega_{\mathbb{k}\wedge\Psi}} Cd\xi - \Big\{\int_0^{\Omega_{\mathbb{k}\wedge\Psi}} \sigma_1dB_1(\xi) \\ &+ \int_0^{\Omega_{\mathbb{k}\wedge\Psi}} \sigma_2dB_2(\xi) + \int_0^{\Omega_{\mathbb{k}\wedge\Psi}} \sigma_3dB_3(\xi) \end{aligned}$$

$$+\int_0^{\Omega_{\Bbbk\wedge\Psi}}\sigma_4 dB_4(\xi)\Big\},$$

using the fact that $\Omega_{\Bbbk\wedge\Psi}=\min\{\Omega_{\mathrm{n}},\xi\}$. Implementing the expectation on the aforesaid variants gives

$$\begin{aligned}\mathcal{V}\big(\mathbf{Y}(\Omega_{\Bbbk\wedge\Psi})\big) &\le \mathcal{V}(\mathbf{Y}(0))+C\int_0^{\Omega_{\Bbbk\wedge\Psi}}d\xi-\Big\{\int_0^{\Omega_{\Bbbk\wedge\Psi}}\sigma_1 dB_1(\xi)\\&+\int_0^{\Omega_{\Bbbk\wedge\Psi}}\sigma_2 dB_2(\xi)+\int_0^{\Omega_{\Bbbk\wedge\Psi}}\sigma_3 dB_3(\xi)\\&+\int_0^{\Omega_{\Bbbk\wedge\Psi}}\sigma_4 dB_4(\xi)\Big\}.\end{aligned}$$

This implies that

$$\mathcal{E}\mathcal{V}\big(\mathbf{Y}(\Omega_{\Bbbk\wedge\Psi})\big)\le\mathcal{V}(\mathbf{Y}(0))+C\mathcal{E}\le\mathcal{V}(\mathbf{Y}(0))+C\Psi. \tag{14}$$

As $\mathcal{V}\big(\mathbf{Y}(\Omega_{\Bbbk\wedge\Psi})\big)>0$, then

$$\begin{aligned}\mathcal{E}\mathcal{V}\big(\mathbf{Y}(\Omega_{\Bbbk\wedge\Psi})\big)&=\mathcal{E}\big[\mathcal{V}\big(\mathbf{Y}(\Omega_{\Bbbk\wedge\Psi})\big)_{\mathbf{x}(\Omega_{\Bbbk}\le\Psi)}\big]+\mathcal{E}\big[\mathcal{V}\big(\mathbf{Y}(\Omega_{\Bbbk\wedge\Psi})\big)_{\mathbf{x}(\Omega_{\Bbbk}>\Upsilon)}\big]\\&\ge\mathcal{E}\big[\mathcal{V}\big(\mathbf{Y}(\Omega_{\Bbbk\wedge\Psi})\big)_{\mathbf{x}(\Omega_{\Bbbk}\le\Psi)}\big].\end{aligned} \tag{15}$$

Further, for $\Omega_{\Bbbk}$, since certain factors of $\mathbf{Y}(\Omega_{\Bbbk}), say\ \ (\mathbf{S}(\Omega_{\Bbbk}))$ including $0<\mathbf{S}(\Omega_{\Bbbk})\le\frac{1}{\Bbbk}<1$.

Thus, $\mathcal{V}(\mathbf{Y}(\Omega_{\Bbbk}))\ge-\ln\Big(\frac{1}{\Bbbk}\Big)$, this allow us to write $\mathcal{V}(\mathbf{Y}(\Omega_{\Bbbk}))=\ln\big(\mathbf{S}(\Omega_{\Bbbk})\big)\le\ln\Big(\frac{1}{\Bbbk}\Big)$.

As a result, from (15) and the previous expression, we have

$$\begin{aligned}\mathcal{E}\mathcal{V}\big(\mathbf{Y}(\Omega_{\Bbbk\wedge\Psi})\big)&\ge\mathcal{E}\big[\mathcal{V}\big(\mathbf{Y}(\Omega_{\Bbbk\wedge\Psi})\big)_{\mathbf{x}(\Omega_{\Bbbk}\le\Psi)}\big]\\&\ge\Big\{-\ln\Big(\frac{1}{\Bbbk}\Big)\Big\}.\end{aligned} \tag{16}$$

Combining (14)–(16), we have

$$\mathcal{E}\mathcal{V}\big(\mathbf{Y}(\Omega_{\Bbbk\wedge\Psi})\big)\ge-\ln\Big(\frac{1}{\Bbbk}\Big)\mathbf{P}(\Omega_{\Bbbk\wedge\Psi}). \tag{17}$$

It follows that

$$\begin{aligned}\mathbf{P}(\Omega_{\Bbbk\wedge\Psi})&\le\frac{\mathcal{E}\mathcal{V}\big(\mathbf{Y}(\Omega_{\Bbbk\wedge\Psi})\big)}{\ln\Bbbk}\\&\le\frac{\mathcal{V}\big(\mathbf{Y}(0)\big)+C\Psi}{\ln\Bbbk}..\end{aligned}$$

Applying limit sup $\Bbbk\mapsto\infty$ on (17), $\forall\ \Psi>0$, we find

$$\mathbf{P}(\Omega_{\Bbbk\wedge\Psi})\le0\quad\Longrightarrow\lim_{\xi\mapsto\infty}\mathbf{P}(\Omega_{\Bbbk\wedge\Psi})=0.$$

This is the desired result. □

Basic reproduction number $(\mathbb{R}_0^{\mathbf{S}})$

Here, the fundamental reproductive factor in this case is the mean value of secondary infectious diseases generated by an infectious person during his contagious phase. In addition, we intend to demonstrate that stochastic $(\mathbb{R}_0^{\mathbf{S}})$ reproduction is a distinct type of fundamental reproduction.

Firstly, in view of the second cohort of system's (10), that is

$$d\mathbf{I}(\xi)=\big(\vartheta\varsigma\mathbf{S}\mathbf{I}+\gamma\vartheta\rho_2\mathbf{V}\mathbf{I}-(\delta_1+\delta_2+\zeta)\mathbf{I}\big)d\xi+\sigma_3\mathbf{I}dB_3(\xi). \tag{18}$$

Considering the Itô's technique for twice differentiation mapping $\mathbf{F}(\mathbf{I})=\ln(\mathbb{I})$, the Taylor series representation is

$$d\mathbf{F}(\xi,\mathbf{I}(\xi))=\frac{\partial\mathbf{F}}{\partial\xi}d\xi+\frac{\partial\mathbf{F}}{\partial\mathbf{I}}d\mathbf{I}+\frac{1}{2}\frac{\partial^2\mathbf{F}}{\partial\mathbf{I}^2}(d\mathbf{I})^2+\frac{\partial^2\mathbf{F}}{\partial\mathbf{I}\partial\xi}d\xi d\mathbf{I}+\frac{1}{2}\frac{\partial^2\mathbf{F}}{\partial\xi^2}(d\xi)^2.$$

This implies that

$$\begin{aligned}d\mathbf{F}(\xi,\mathbf{I}(\xi))&=\frac{1}{\mathbf{I}(\xi)}\Big\{\big(\vartheta\varsigma\mathbf{S}\mathbf{I}+\gamma\vartheta\rho_2\mathbf{V}\mathbf{I}-(\delta_1+\delta_2+\zeta)\mathbf{I}\big)d\xi+\sigma_3\mathbf{I}dB_3(\xi)\Big\}\\&-\frac{1}{2\mathbf{I}^2(\xi)}\Big\{\big(\vartheta\varsigma\mathbf{S}\mathbf{I}+\gamma\vartheta\rho_2\mathbf{V}\mathbf{I}-(\delta_1+\delta_2+\zeta)\mathbf{I}\big)d\xi+\sigma_3\mathbf{I}dB_3(\xi)\Big\}^2\\&+\frac{\partial\mathbf{F}}{\partial\xi\partial\mathbf{I}}d\xi\Big\{\frac{1}{\mathbf{I}(\xi)}\Big\{\big(\vartheta\varsigma\mathbf{S}\mathbf{I}+\gamma\vartheta\rho_2\mathbf{V}\mathbf{I}-(\delta_1+\delta_2+\zeta)\mathbf{I}\big)d\xi\\&+\sigma_3\mathbf{I}dB_3(\xi)\Big\}\Big\}.\end{aligned}$$

It follows that

$$\begin{aligned}d\mathbf{F}(\xi,\mathbf{I}(\xi))&=\Big\{\big(\vartheta\varsigma\mathbf{S}+\gamma\vartheta\rho_2\mathbf{V}-(\delta_1+\delta_2+\zeta)\big)d\xi+\sigma_3dB_3(\xi)\Big\}\\&-\frac{1}{2\mathbf{I}^2(\xi)}\Big\{\mathcal{A}_1^2(d\xi)^2+2\mathcal{A}_1\mathcal{A}_2d\xi dB_2(\xi)+\mathcal{A}_2^2(dB_2(\xi))^2\Big\},\end{aligned}$$

where $\mathcal{A}_1=\vartheta\varsigma\mathbf{S}\mathbf{I}+\gamma\vartheta\rho_2\mathbf{V}\mathbf{I}-(\delta_1+\delta_2+\zeta)\mathbf{I}$ and $\mathcal{A}_2=\sigma_3\mathbf{I}$, then can be written as

$$\begin{aligned}d\mathbf{F}(\xi,\mathbf{I}(\xi))&=\Big\{\big(\vartheta\varsigma\mathbf{S}+\gamma\vartheta\rho_2\mathbf{V}-(\delta_1+\delta_2+\zeta)\big)d\xi+\sigma_3dB_3(\xi)\Big\}\\&-\frac{1}{2\mathbf{I}^2(\xi)}\Big\{\mathcal{A}_2^2(dB_2(\xi))^2\Big\}\\&=\Big\{\big(\vartheta\varsigma\mathbf{S}+\gamma\vartheta\rho_2\mathbf{V}-(\delta_1+\delta_2+\zeta)\big)d\xi+\sigma_3dB_3(\xi)\Big\}\\&-\frac{1}{2\mathbf{I}^2(\xi)}\Big\{(\sigma_3\mathbf{I})^2\Big\}d\xi.\end{aligned} \tag{19}$$

As $d\xi\mapsto0$, $(d\xi)^2$, $d\xi dB_2(\xi)\mapsto0$ and $(dB_2(\xi))^2$ can be converted to $d\xi$ (By the variance of Wiener technique), we have

$$\begin{aligned}&d\mathbf{F}(\xi,\mathbf{I}(\xi))\\&=\Big\{\big(\vartheta\varsigma\mathbf{S}+\gamma\vartheta\rho_2\mathbf{V}-(\delta_1+\delta_2+\zeta)\big)d\xi+\sigma_3dB_3(\xi)\Big\}-\frac{1}{2}(\sigma_3)^2d\xi\\&=\Big\{\big(\vartheta\varsigma\mathbf{S}+\gamma\vartheta\rho_2\mathbf{V}-(\delta_1+\delta_2+\zeta)\big)d\xi-\frac{1}{2}(\sigma_3)^2\Big\}d\xi+\sigma_3dB_3(\xi)\\&=\Big\{\big(\vartheta\varsigma\mathbf{S}+\gamma\vartheta\rho_2\mathbf{V}-\frac{1}{2}(\sigma_3)^2\big)-(\delta_1+\delta_2+\zeta)\Big\}d\xi+\sigma_3dB_3(\xi).\end{aligned} \tag{20}$$

Taking into consideration the next generation matrices [39] are as follows

$$\mathbf{F}=\vartheta\varsigma\mathbf{S}+\gamma\vartheta\rho_2\mathbf{V}-\frac{1}{2}(\sigma_3)^2\ \ and\ \ \mathbf{V}=\delta_1+\delta_2+\zeta.$$

Therefore, $\mathbf{F}$ and $\mathbf{V}$ at disease-free equilibrium $\mathcal{E}_0=\Big(\frac{\big((1-\mathbf{q})+b/\delta_1\big)\pi}{\delta_1+\rho_1},\frac{\mathbf{q}\pi}{\delta_1+\rho_1},0,0\Big)$, we find

$$\mathbf{F}=\vartheta\varsigma\frac{\big((1-\mathbf{q})+b/\delta_1\big)\pi}{\delta_1+\rho_1}+\gamma\vartheta\rho_2\frac{\mathbf{q}\pi}{\delta_1+\rho_1}-\frac{1}{2}(\sigma_3)^2\ \ and\ \ \mathbf{V}=\delta_1+\delta_2+\zeta.$$

The characteristic polynomial can be written as

$$\left|\frac{\vartheta\varsigma\pi\big((1-\mathbf{q})+\rho_1/\delta_1+\gamma\mathbf{q}\big)}{(\rho_1+\delta_1)(\delta_1+\delta_2+\zeta)}-\frac{\sigma_3^2}{2(\delta_1+\delta_2+\zeta)}-\lambda\right|=0.$$

This yields

$$\lambda=\frac{\vartheta\varsigma\pi\big((1-\mathbf{q})+\rho_1/\delta_1+\gamma\mathbf{q}\big)}{(\rho_1+\delta_1)(\delta_1+\delta_2+\zeta)}-\frac{\sigma_3^2}{2(\delta_1+\delta_2+\zeta)}.$$

According to the [39] approach, the dominating eigenvalue is the $\mathbb{R}_0^{\mathbf{S}}$. Thus

$$\mathbb{R}_0^{\mathbf{S}}=\frac{\vartheta\varsigma\pi\big((1-\mathbf{q})+\rho_1/\delta_1+\gamma\mathbf{q}\big)-\sigma_3^2}{2(\rho_1+\delta_1)(\delta_1+\delta_2+\zeta)},$$

which is the required stochastic fundamental reproduction number.

Local stability of diseases-free equilibrium point (DFEP) in stochastic sense

Theorem 2. *For a community's infection to be eradicated, then* $\mathbb{R}_0^{\mathbf{S}}<1$.

If $\mathbb{R}_0^{\mathbf{S}}<1$, *then for any provided ICs* $\big(\mathbf{S}(0),\mathbf{V}(0),\mathbf{I}(0),\mathbf{R}(0)\big)=\big(\mathbf{S}_0,\mathbf{V}_0,\mathbf{I}_0,\mathbf{R}_0\big)\in\mathbb{R}_+^4$. *Therefore,* $\mathbf{I}(\xi)$ *admits* $\lim_{\xi\mapsto\infty}\sup\frac{\ln(\mathbf{I}(\xi))}{\xi}\le(\delta_1+\delta_2+\zeta)(\mathbb{R}_0^{\mathbf{S}}-1)$ *almost surely.*

Proof. Taking into consideration (18), we have

$$d\mathbf{F}(\xi,\mathbf{I}(\xi))=\big(\vartheta\varsigma\mathbf{S}+\gamma\vartheta\rho_2\mathbf{V}-\frac{1}{2}\sigma_3^2-(\delta_1+\delta_2+\zeta)\big)d\xi+\sigma_3dB_3(\xi).$$

It follows that

$$d\ln(\mathbf{I})=\big(\vartheta\varsigma\mathbf{S}+\gamma\vartheta\rho_2\mathbf{V}-\frac{1}{2}\sigma_3^2-(\delta_1+\delta_2+\zeta)\big)d\xi+\sigma_3dB_3(\xi).$$

After performing integration, we have

$$\begin{aligned}\ln(\mathbf{I}) &= \ln(\mathbf{I}_0) + \int_0^{\xi} \left(\vartheta\varsigma\mathbf{S} + \gamma\vartheta\rho_2\mathbf{V} - \frac{1}{2}\sigma_3^2 - (\delta_1+\delta_2+\zeta)\right)d\xi \\ &\quad + \sigma_3\int_0^{\xi} dB_3(\xi) \\ &\le \ln(\mathbf{I}_0) + \underbrace{\left(\vartheta\varsigma\frac{\pi\left((1-\mathbf{q})+\rho_1/\delta_1+\gamma\mathbf{q}\right)}{\delta_1+\rho_1} - \frac{1}{2}\sigma_3^2 - (\delta_1+\delta_2+\zeta)\right)\xi}_{at\ \ DFEP\ \ \mathcal{E}_0} \\ &\quad + \sigma_3\int_0^{\xi} dB_3(\xi) \\ &\le \ln(\mathbf{I}_0) + \left(\vartheta\varsigma\frac{\pi\left((1-\mathbf{q})+\rho_1/\delta_1+\gamma\mathbf{q}\right)}{\delta_1+\rho_1} - \frac{1}{2}\sigma_3^2 - (\delta_1+\delta_2+\zeta)\right)\xi \\ &\quad + \Lambda(\xi), \end{aligned} \tag{21}$$

where $\Lambda(\xi) = \sigma_3\int_0^{\xi} dB_3(\xi)$ is the martingale. therefore, by the strong principal of large values for $\Lambda(\xi)$, see [40], we get $\lim_{\xi\mapsto\infty}\sup\frac{\Lambda(\xi)}{\xi} = 0$ almost probably.

After dividing by ξ and applying limit $\xi \mapsto \infty$, then (21) reduces to

$$\begin{aligned}\lim_{\xi\mapsto\infty}\sup\frac{\ln(\mathbf{I})}{\xi} &\le \vartheta\varsigma\frac{\pi\left((1-\mathbf{q})+\rho_1/\delta_1+\gamma\mathbf{q}\right)}{\delta_1+\rho_1} - \frac{1}{2}\sigma_3^2 - (\delta_1+\delta_2+\zeta) \\ &= (\delta_1+\delta_2+\zeta)\left(\vartheta\varsigma\frac{\pi\left((1-\mathbf{q})+\rho_1/\delta_1+\gamma\mathbf{q}\right)}{(\delta_1+\rho_1)(\delta_1+\delta_2+\zeta)} \right. \\ &\quad \left. - \frac{1}{2(\delta_1+\delta_2+\zeta)}\sigma_3^2\right) \\ &= (\delta_1+\delta_2+\zeta)(\mathbb{R}_0^{\mathbf{S}}-1) < 0.\end{aligned}$$

This indicates that $\mathbb{R}_0^{\mathbf{S}} < 1$.

Finally, $\mathbb{R}_0^{\mathbf{S}}$ should be smaller than 1 for disease elimination in a population. □

Theorem 3. *For prevalence of disease in the population $\mathbb{R}_0^{\mathbf{S}} > 1$. If $\mathbb{R}_0^{\mathbf{S}} > 1$, therefore for the provided initial data $\mathbf{I}(0) \in (0, \pi/d_1)$, then the solution of (10) admits*

$$\lim_{\xi\mapsto\infty}\sup(\mathbf{I}(\xi)) \ge \eta \tag{22}$$

almost probably, where η is the root of $h_1(\mathbf{I}) = \vartheta\varsigma(\mathbf{N}-(\mathbf{V}+\mathbf{I}+\mathbf{R}))+\gamma\vartheta\varsigma(\mathbf{N}-(\mathbf{S}+\mathbf{I}+\mathbf{R})) - \frac{\sigma_3^2}{2} - (\delta_1+\delta_2+\zeta) = 0$.

Proof. Since $\mathbb{R}_0^{\mathbf{S}} > 1$, we have

$$\begin{aligned}h_1(0) &= \vartheta\varsigma(\mathbf{N}-(\mathbf{V}+\mathbf{R})) + \gamma\vartheta\varsigma(\mathbf{N}-(\mathbf{S}+\mathbf{R})) - \frac{\sigma_3^2}{2} - (\delta_1+\delta_2+\zeta) \\ &= \underbrace{\vartheta\varsigma\frac{\pi\left((1-\mathbf{q})+\rho_1/\delta_1+\gamma\mathbf{q}\right)}{(\rho_1+\delta_1)}}_{at\ \ DFEP\ \ \mathcal{E}_0} - \frac{\sigma_3^2}{2} - (\delta_1+\delta_2+\zeta) \\ &= (\delta_1+\delta_2+\zeta)\left\{\vartheta\varsigma\frac{\pi\left((1-\mathbf{q})+\rho_1/\delta_1+\gamma\mathbf{q}\right)}{(\rho_1+\delta_1)} - \frac{\sigma_3^2}{2(\delta_1+\delta_2+\zeta)} - 1\right\} \\ &= (\delta_1+\delta_2+\zeta)(\mathbb{R}_0^{\mathbf{S}}-1) > 0.\end{aligned}$$

Also, we have

$$\begin{aligned}h_1(\mathbf{N}) &= -\vartheta\varsigma(\mathbf{V}+\mathbf{R}) - \gamma\vartheta\varsigma(\mathbf{S}+\mathbf{R}) - \frac{\sigma_3^2}{2} - (\delta_1+\delta_2+\zeta) \\ &= -\vartheta\varsigma\mathbf{S} - \gamma\vartheta\varsigma\mathbf{V} - \frac{\sigma_3^2}{2} - (\delta_1+\delta_2+\zeta) \\ &= -(\delta_1+\delta_2+\zeta)\left\{\vartheta\varsigma\frac{\pi\left((1-\mathbf{q})+\rho_1/\delta_1+\gamma\mathbf{q}\right)}{(\rho_1+\delta_1)(\delta_1+\delta_2+\zeta)} + \frac{\sigma_3^2}{2(\delta_1+\delta_2+\zeta)} + 1\right\} \\ &= -(\delta_1+\delta_2+\zeta)\left(\mathbb{R}_0^{\mathbf{S}} + \frac{\sigma_3^2}{2(\delta_1+\delta_2+\zeta)} + 1\right) \\ &= -(\delta_1+\delta_2+\zeta)\left((\mathbb{R}_0^{\mathbf{S}}+1) + \frac{\sigma_3^2}{2(\delta_1+\delta_2+\zeta)}\right) < 0.\end{aligned}$$

Then $h_1(\mathbf{I})$ permits a zero $\eta \in (0, \pi/d_1)(0,\ \mathrm{d})$, and since $h_1(\mathbf{I})$ is decreasing about η, we can simply illustrate that we have for every substantially significant $\epsilon > 0$, one can find

$$h_1(\eta+\epsilon) < 0 < h_1(\eta-\epsilon). \tag{23}$$

We are now able to back up our claim (23). If this is not the case, then there is a relatively small $\epsilon > 0$ so that $p(\nabla_1) > 0$ where $\nabla_1 = \left\{\lim_{\xi\mapsto\infty}\sup(\mathbf{I}(\xi)) \le \eta - 2\epsilon\right\}$, and so there is $\varpi \in \nabla_1$ such that for every $\varpi \in \nabla_1$ there is $T(\varpi) > 0$ such that

$$0 \le \mathbf{I}(\xi,\varpi) \le h_1(\eta-\epsilon), \quad \forall\ \xi \ge T(\varpi). \tag{24}$$

As a consequence of (23) and (24), it concludes that

$$h_1(\mathbf{I}(\xi,\varpi)) \le h_1(\eta-\epsilon), \quad \forall\ \xi \ge T(\varpi). \tag{25}$$

Furthermore, according to the strong rule of large vales for martingales, there is a $\nabla_2 \subset \nabla$ having $p(\nabla_2) = 1$ such that $\varpi \in \nabla_2\ \lim_{\xi\mapsto\infty}\sup\frac{\Lambda(\xi)}{\xi} = 0$ almost probably.

Now, make the necessary adjustments $\varpi \in \nabla_1 \cap \nabla_2$, then utilizing (25), so that for $\xi \ge T(\varpi)$,

$$\begin{aligned}\ln\mathbf{I}(\xi,\varpi) &= \ln\mathbf{I}(0) + \int_0^{T(\varpi)} h_1(\mathbf{I}(s_1))ds_1 + \int_{T(\varpi)}^{\xi} h_1(\mathbf{I}(s_1))ds_1 + \Lambda(\xi) \\ &\ge \ln\mathbf{I}(0) + \int_0^{T(\varpi)} h_1(\mathbf{I}(s_1))ds_1 + h_1(\eta-\epsilon)(\xi - T(\varpi))ds_1 + \Lambda(\xi).\end{aligned}$$

This gives $\lim_{\xi\mapsto\infty}\inf\frac{\ln\mathbf{I}(\xi,\varpi)}{\xi} > h_1(\eta-\epsilon)$, where $\lim_{\xi\mapsto\infty}\ln\mathbf{I}(\xi,\varpi) = \infty$.

This contradicting (23), hence the prescribed assumption (22) should always true, that is., $\lim_{\xi\mapsto\infty}\sup(\mathbf{I}(\xi)) \ge \eta$ almost probably. □

Existence-uniqueness of the solution

Now, the model's (10) existence and uniqueness criteria are provided. To do so, we demonstrate that $(\boldsymbol{\Phi}_l(\xi,x_l))_{l\in[1,2,3,4]}$ and $(\mathcal{W}_l(\xi,x_l))_{l\in[1,2,3,4]}$

$$\left|\rho_l(\xi,x_l)\right|.\ \left|\mathcal{W}_l(\xi,x_l)\right| < \kappa_l(1+\left|x_l\right|^2),\quad \forall \tag{26}$$

$$\xi \in [0,T], \tag{27}$$

and

$$\left|\boldsymbol{\Phi}_l(\xi,x_l^1)-\boldsymbol{\Phi}_l(\xi,x_l^1)\right|^2,\ \left|\mathcal{W}_l(\xi,x_l^1)-\mathcal{W}_l(\xi,x_l^1)\right|^2 < \tilde{\kappa}_l\left|x_l^1-x_l^2\right|,\quad \forall\ \xi\in[0,T]. \tag{28}$$

The system (10) can be expressed as

$$\begin{cases} d\mathbf{S}(\xi) = \boldsymbol{\Phi}_1(\mathbf{S},\xi)d\xi + \sigma_1\mathcal{W}_1(\mathbf{S},\xi)B_1(\xi), \\ d\mathbf{V}(\xi) = \boldsymbol{\Phi}_2(\mathbf{V},\xi)d\xi + \sigma_2\mathcal{W}_2(\mathbf{V},\xi)B_2(\xi), \\ d\mathbf{I}(\xi) = \boldsymbol{\Phi}_3(\mathbf{I},\xi)d\xi + \sigma_3\mathcal{W}_3(\mathbf{I},\xi)B_3(\xi), \\ d\mathbf{R}(\xi) = \boldsymbol{\Phi}_4(\mathbf{R},\xi)d\xi + \sigma_4\mathcal{W}_4(\mathbf{R},\xi)B_4(\xi). \end{cases} \tag{29}$$

Let us introduce

$$\left\|\rho\right\|_{\infty} = \sup_{\xi\in D_{q_1}}\left|\rho(\xi)\right|. \tag{30}$$

For every $\xi \in [0,T]$, we attain

$$\begin{aligned}\left|\boldsymbol{\Phi}_1(\mathbf{S},\xi)\right|^2 &= \left|(1-\mathbf{q})\pi + \rho_1\mathbf{V} + \chi\mathbf{R} - \delta_1\mathbf{S} - \vartheta\rho_2\mathbf{S}\mathbf{I}\right|^2 \\ &\le 2(1-\mathbf{q})^2\pi^2 + 2\left|\rho_1\mathbf{V} + \chi\mathbf{R} - (\delta_1+\vartheta\rho_2\mathbf{I})\right|^2\left|\mathbf{S}\right|^2 \\ &\le 2(1-\mathbf{q})^2\pi^2 + \left(8\rho_1\left|\mathbf{V}\right|^2 + 4\chi^2\left|\mathbf{R}\right|^2 + 8\mu^2 + 8\vartheta^2\rho_2^2\mathbf{I}\right)\left|\mathbf{S}\right|^2 \\ &\le 2(1-\mathbf{q})^2\pi^2 + \left(8\rho_1\sup_{\xi\in[0,T]}\left|\mathbf{V}\right|^2 + 4\chi^2\sup_{\xi\in[0,T]}\left|\mathbf{R}\right|^2\right. \\ &\quad \left. + 8\mu^2 + 8\vartheta^2\rho_2^2\sup_{\xi\in[0,T]}\left|\mathbf{I}\right|^2\right)\left|\mathbf{S}\right|^2 \\ &\le 2(1-\mathbf{q})^2\pi^2\end{aligned}$$

$$\times\left(1+\frac{8\rho_1\left\|\mathbf{V}\right\|_\infty^2+4\chi^2\left\|\mathbf{R}\right\|_\infty^2+8\mu^2+8\vartheta^2\rho_2^2\left\|\mathbf{I}\right\|_\infty^2}{2(1-\mathbf{q})^2\pi^2}\left|\mathbf{S}\right|^2\right)$$
$$\leq \kappa_1(1+\left|\mathbf{S}\right|^2) \tag{31}$$

such that $\frac{8\rho_1\left\|\mathbf{V}\right\|_\infty^2+4\chi^2\left\|\mathbf{R}\right\|_\infty^2+8\mu^2+8\vartheta^2\rho_2^2\left\|\mathbf{I}\right\|_\infty^2}{2(1-\mathbf{q})^2\pi^2} < 1$ and $\kappa_1 = 2(1-\mathbf{q})^2\pi^2$. Analogously, we find

$$\begin{aligned}\left|\boldsymbol{\Phi}_2(\mathbf{V},\xi)\right|^2 &\leq 3\mathbf{q}^2\pi^2+\left(6\gamma^2\rho_2^2\vartheta^2\left\|\mathbf{I}\right\|_\infty^2+6(\rho_1+\delta_1)^2\right)\left|\mathbf{V}\right|^2\\ &\leq 3\mathbf{q}^2\pi^2\left(1+\frac{6\gamma^2\rho_2^2\vartheta^2\left\|\mathbf{I}\right\|_\infty^2+6(\rho_1+\delta_1)^2}{3\mathbf{q}^2\pi^2}\left|\mathbf{V}\right|^2\right)\\ &\leq \kappa_2(1+\left|\mathbf{V}\right|^2),\end{aligned} \tag{32}$$

where $\kappa_2 = \frac{6\gamma^2\rho_2^2\vartheta^2\left\|\mathbf{I}\right\|_\infty^2+6(\rho_1+\delta_1)^2}{3\mathbf{q}^2\pi^2}$. Furthermore, we have

$$\begin{aligned}\left|\boldsymbol{\Phi}_3(\mathbf{I},\xi)\right|^2 &\leq 3\left(\vartheta^2\varsigma^2\left\|\mathbf{S}\right\|_\infty^2+\gamma^2\vartheta^2\rho_2^2\left\|\mathbf{V}\right\|_\infty^2-(\delta_1+\delta_2+\zeta)^2\right)\left|\mathbf{I}\right|^2\\ &\leq 3\left(\vartheta^2\varsigma^2\left\|\mathbf{S}\right\|_\infty^2+\gamma^2\vartheta^2\rho_2^2\left\|\mathbf{V}\right\|_\infty^2-(\delta_1+\delta_2+\zeta)^2\right)(1+\left|\mathbf{I}\right|^2)\\ &\leq \kappa_3(1+\left|\mathbf{I}\right|^2),\end{aligned} \tag{33}$$

where $\kappa_3 = 3\left(\vartheta^2\varsigma^2\left\|\mathbf{S}\right\|_\infty^2+\gamma^2\vartheta^2\rho_2^2\left\|\mathbf{V}\right\|_\infty^2-(\delta_1+\delta_2+\zeta)^2\right)$.

Again, we have

$$\begin{aligned}\left|\boldsymbol{\Phi}_4(\mathbf{R},\xi)\right|^2 &\leq 2\left(\zeta^2\left\|\mathbf{I}\right\|_\infty^2+(\chi+\delta_1)^2\right)\left|\mathbf{R}\right|^2\\ &\leq 2\left(\zeta^2\left\|\mathbf{I}\right\|_\infty^2+(\chi+\delta_1)^2\right)(1+\left|\mathbf{R}\right|^2)\\ &\leq \kappa_4(1+\left|\mathbf{R}\right|^2),\end{aligned} \tag{34}$$

where $\kappa_4 = \left(\zeta^2\left\|\mathbf{I}\right\|_\infty^2+(\chi+\delta_1)^2\right)$. For every $\xi\in[0,T]$, we have

$$\begin{aligned}&\left|\mathcal{W}_1(\mathbf{S},\xi)\right|^2 = \sigma_1^2\left|\mathbf{S}\right|^2 \leq \sigma_1^2(1+\left|\mathbf{S}\right|^2),\\ &\left|\mathcal{W}_2(\mathbf{V},\xi)\right|^2 \leq \sigma_2^2(1+\left|\mathbf{V}\right|^2),\\ &\left|\mathcal{W}_3(\mathbf{I},\xi)\right|^2 \leq \sigma_3^2(1+\left|\mathbf{V}\right|^2),\\ &\left|\mathcal{W}_4(\mathbf{R},\xi)\right|^2 \leq \sigma_4^2(1+\left|\mathbf{R}\right|^2).\end{aligned} \tag{35}$$

Now, we illustrate the Lipschitz assumption for $(\boldsymbol{\Phi}_i(\xi,x_i))_{i\in[1,2,3,4]}$ and $(\mathcal{W}_i(\xi,x_i))_{i\in[1,2,3,4]}$

$$\begin{aligned}\left|\boldsymbol{\Phi}_1(\xi,\mathbf{S}_1)-\boldsymbol{\Phi}_1(\xi,\mathbf{S}_2)\right|^2 &= \left|-\delta_1-\vartheta\rho_2\mathbf{I}\right|^2\left|\mathbf{S}_1-\mathbf{S}_2\right|^2\\ &\leq \left(2\delta_1^2+2\vartheta^2\rho_2^2\left\|\mathbf{I}^2\right\|_\infty^2\right)\left|\mathbf{S}_1-\mathbf{S}_2\right|^2\\ &\leq \tilde{\kappa_1}\left|\mathbf{S}_1-\mathbf{S}_2\right|^2,\end{aligned}$$

$$\begin{aligned}\left|\boldsymbol{\Phi}_2(\xi,\mathbf{V}_1)-\boldsymbol{\Phi}_2(\xi,\mathbf{V}_2)\right|^2 &= \left|-\gamma\vartheta\rho_2\mathbf{I}-(\rho_1+\delta_1)\right|^2\left|\mathbf{V}_1-\mathbf{V}_2\right|^2\\ &\leq \left(2\gamma^2\vartheta^2\rho_2^2\left\|\mathbf{I}^2\right\|_\infty^2+2(\rho_1+\delta_1)\right)\left|\mathbf{V}_1-\mathbf{V}_2\right|^2\\ &\leq \tilde{\kappa_2}\left|\mathbf{V}_1-\mathbf{V}_2\right|^2,\end{aligned}$$

$$\begin{aligned}\left|\boldsymbol{\Phi}_3(\xi,\mathbf{I}_1)-\boldsymbol{\Phi}_3(\xi,\mathbf{I}_2)\right|^2 &= \left|\vartheta\varsigma\mathbf{S}+\gamma^2\vartheta^2\rho_2^2\mathbf{V}-(\delta_1+\delta_2+\zeta)\right|^2\left|\mathbf{I}_1-\mathbf{I}_2\right|^2\\ &\leq \left(3\vartheta^2\varsigma^2\left\|\mathbf{S}^2\right\|_\infty^2+3\gamma^2\vartheta^2\rho_2^2\left\|\mathbf{V}^2\right\|_\infty^2\right.\\ &\quad\left.+3(\delta_1+\delta_2+\zeta)^2\right)\left|\mathbf{I}_1-\mathbf{I}_2\right|^2\\ &\leq \tilde{\kappa_3}\left|\mathbf{I}_1-\mathbf{I}_2\right|^2,\end{aligned}$$

$$\begin{aligned}\left|\boldsymbol{\Phi}_4(\xi,\mathbf{R}_1)-\boldsymbol{\Phi}_4(\xi,\mathbf{R}_2)\right|^2 &= \left|\zeta\mathbf{I}-(\chi+\delta_1)\right|^2\left|\mathbf{R}_1-\mathbf{R}_2\right|^2\\ &\leq \left(2\zeta^2\left\|\mathbf{I}^2\right\|_\infty^2+2(\chi+\delta_1)\right)\left|\mathbf{R}_1-\mathbf{R}_2\right|^2\\ &\leq \tilde{\kappa_4}\left|\mathbf{R}_1-\mathbf{R}_2\right|^2,\end{aligned}$$

Thus, if the assumption on linear growth satisfies

$$\begin{aligned}\min\Bigg\{&\frac{8\rho_1\left|\mathbf{V}\right|_\infty^2+4\chi^2\left\|\mathbf{R}\right|_\infty^2+8\mu^2+8\vartheta^2\rho_2^2\left\|\mathbf{I}\right|_\infty^2}{2(1-\mathbf{q})^2\pi^2},\frac{6\gamma^2\rho_2^2\vartheta^2\left\|\mathbf{I}\right\|_\infty^2+6(\rho_1+\delta_1)^2}{3\mathbf{q}^2\pi^2},\\ &3\left(\vartheta^2\varsigma^2\left\|\mathbf{S}\right\|_\infty^2+\gamma^2\vartheta^2\rho_2^2\left\|\mathbf{V}\right\|_\infty^2-(\delta_1+\delta_2+\zeta)^2\right),\left(\zeta^2\left\|\mathbf{I}\right\|_\infty^2+(\chi+\delta_1)^2\right)\Bigg\}\\ &<1.\end{aligned} \tag{36}$$

Both two assumption are verified. So according to the above hypothesis, then system (10) has unique solution.

Extinction of infection

In this part, we will analyse how the eradication of infectious species is explained. To do so, we formulated a functional as

$$\langle\mathbf{y}(\xi)\rangle = \frac{1}{\xi}\int_0^\xi \mathbf{y}(\tau)d\tau.$$

Theorem 4. *Suppose there be a assumption* $\delta_1 < \frac{\sigma_1^2\sigma_2^2\sigma_3^2\sigma_4^2}{2}$ *and* $(\mathbf{S},\mathbf{V},\mathbf{I},\mathbf{R})$ *is the solution of the system (10) considering a further supposition that* $(\mathbf{S}(0),\mathbf{V}(0),\mathbf{I}(0),\mathbf{R}(0))\in\mathbb{R}_+^4$ *and* $\mathbb{R}_0^{\mathbf{S}}<1$, *then* $\lim_{\xi\mapsto\infty}\frac{\langle\log\mathbf{I}(\xi)\rangle}{\xi}<0$. *That yields* $\mathbf{I}(\xi)\mapsto 0$ *exponentially, this means that the infection will dying out with unit probability. Furthermore*

$$\begin{aligned}&\lim_{\xi\mapsto\infty}\frac{1}{\xi}\int_0^\xi \mathbf{S}(\tau)d\tau = \frac{(1-\mathbf{q}+\rho_1/\delta_1)\pi}{\rho_1+\delta_1},\\ &\lim_{\xi\mapsto\infty}\frac{1}{\xi}\int_0^\xi \mathbf{V}(\tau)d\tau = \frac{\mathbf{q}\pi}{\rho_1+\delta_1},\\ &\lim_{\xi\mapsto\infty}\frac{1}{\xi}\int_0^\xi \mathbf{I}(\tau)d\tau = 0,\\ &\lim_{\xi\mapsto\infty}\frac{1}{\xi}\int_0^\xi \mathbf{R}(\tau)d\tau = 0.\end{aligned} \tag{37}$$

Proof. Performing integration to (10) and dividing by ξ gives

$$\begin{aligned}\frac{\mathbf{S}(\xi)-\mathbf{S}(0)}{\xi} &= (1-\mathbf{q})\pi+\rho_1\langle\mathbf{V}\rangle+\chi\langle\mathbf{R}\rangle-\delta_1\langle\mathbf{S}\rangle-\vartheta\rho_2\langle\mathbf{SI}\rangle\\ &\quad+\frac{\sigma_1}{\xi}\int_0^\xi \mathbf{S}(\tau)dB_1(\tau),\\ \frac{\mathbf{V}(\xi)-\mathbf{V}(0)}{\xi} &= \mathbf{q}\pi-\gamma\rho_2\vartheta\langle\mathbf{VI}\rangle-(\rho_1+\delta_1)\langle\mathbf{V}\rangle+\frac{\sigma_2}{\xi}\int_0^\xi \mathbf{V}(\tau)dB_2(\tau),\\ \frac{\mathbf{I}(\xi)-\mathbf{I}(0)}{\xi} &= \vartheta\varsigma\langle\mathbf{SI}\rangle+\gamma\vartheta\rho_2\langle\mathbf{VI}\rangle-(\delta_1+\delta_2+\zeta)\langle\mathbf{I}\rangle+\frac{\sigma_3}{\xi}\int_0^\xi \mathbf{I}(\tau)dB_3(\tau),\\ \frac{\mathbf{R}(\xi)-\mathbf{R}(0)}{\xi} &= \zeta\langle\mathbf{I}\rangle-\chi\langle\mathbf{R}\rangle-\delta_1\langle\mathbf{R}\rangle+\frac{\sigma_4}{\xi}\int_0^\xi \mathbf{R}(\tau)dB_4(\tau).\end{aligned} \tag{38}$$

However, a direct implementation of $\mathbf{I}$ to formula produces

$$d\ln\mathbf{I}(\xi) = \left(\vartheta\varsigma\mathbf{S}+\gamma\vartheta\rho_2\mathbf{V}-\left(\delta_1+\delta_2+\zeta+\frac{\sigma_3^2}{2}\right)\right)+\sigma_3 dB_3(\xi). \tag{39}$$

Performing integration over $(0,\xi)$ and dividing by ξ gives

$$\begin{aligned}\frac{\ln\mathbf{I}(\xi)-\ln\mathbf{I}(0)}{\xi} &= \left(\vartheta\varsigma\langle\mathbf{S}\rangle+\gamma\vartheta\rho_2\langle\mathbf{V}\rangle-\left(\delta_1+\delta_2+\zeta+\frac{\sigma_3^2}{2}\right)\right)\\ &\quad+\frac{\sigma_3}{\xi}\int_0^\xi dB_3(\tau)\\ &\leq \left(\vartheta\varsigma+\gamma\vartheta\rho_2-\left(\delta_1+\delta_2+\zeta+\frac{\sigma_3^2}{2}\right)\right)+\frac{\sigma_3}{\xi}\int_0^\xi dB_3(\tau)\\ &\leq \left(\delta_1+\delta_2+\zeta+\frac{\sigma_3^2}{2}\right)\left(\frac{\vartheta\varsigma+\gamma\vartheta\rho_2}{\left(\delta_1+\delta_2+\zeta+\frac{\sigma_3^2}{2}\right)}-1\right)\\ &\quad+\frac{\sigma_3}{\xi}\int_0^\xi dB_3(\tau)\end{aligned}$$

$$\leq \left(\delta_1+\delta_2+\zeta+\frac{\sigma_3^2}{2}\right)(\mathbb{R}_0^{\mathbf{S}}-1)+\frac{\sigma_3}{\xi}\int_0^{\xi} d\,B_3(\tau), \tag{40}$$

where $M_1(\xi)=\frac{\sigma_3}{\xi}\int_0^{\xi} d\,B_3(\tau)$, which is local continuous Martingale and $M_1(0)=0$, $\lim_{\xi\mapsto\infty}\sup\frac{M_1(\xi)}{\xi}=0$. This, if $\mathbb{R}_0^{\mathbf{S}}<1$, then

$$\lim_{\xi\mapsto\infty}\sup\frac{\ln\mathbf{I}(\xi)}{\xi}\leq\left(\delta_1+\delta_2+\zeta+\frac{\sigma_3^2}{2}\right)(\mathbb{R}_0^{\mathbf{S}}-1)<0. \tag{41}$$

So, we have $\lim_{\xi\mapsto\infty}\langle\mathbf{I}(\xi)\rangle=0$.

For cohort $\mathbf{S}(\xi)$, we have

$$\begin{aligned}
\frac{\mathbf{S}(\xi)-\mathbf{S}(0)}{\xi}&=(1-\mathbf{q})\pi+\rho_1\langle\mathbf{V}\rangle+\chi\langle\mathbf{R}\rangle-\delta_1\langle\mathbf{S}\rangle-\vartheta\rho_2\langle\mathbf{SI}\rangle\\
&+\frac{\sigma_1}{\xi}\int_0^{\xi}\mathbf{S}(\tau)d\,B_1(\tau),\\
\langle\mathbf{S}\rangle&=\frac{(1-\mathbf{q})\pi}{\delta_1}+\frac{1}{\delta_1}\left\{\rho_1\frac{\mathbf{q}\pi}{(\rho_1+\delta_1)}+\chi\langle\mathbf{R}\rangle-\vartheta\rho_2\langle\mathbf{SI}\rangle+\frac{\mathbf{S}(0)-\mathbf{S}(\xi)}{\xi}\right.\\
&\left.+\frac{\sigma_1}{\xi}\int_0^{\xi}\mathbf{S}(\tau)d\,B_1(\tau)\right\},
\end{aligned} \tag{42}$$

which yields $\lim_{\xi\mapsto\infty}\langle\mathbf{S}(\xi)\rangle=\frac{(1-\mathbf{q}+\rho_1/\delta_1)\pi}{\rho_1+\delta_1}$.

Furthermore,for cohort $\mathbf{V}(\xi)$, we have

$$\langle\mathbf{V}\rangle=\frac{\mathbf{q}\pi}{(\rho_1+\delta_1)}-\frac{1}{(\rho_1+\delta_1)}\left\{\gamma\rho_2\vartheta\langle\mathbf{VI}\rangle-\frac{\mathbf{V}(0)-\mathbf{V}(\xi)}{\xi}+\frac{\sigma_2}{\xi}\int_0^{\xi}\mathbf{V}(\tau)d\,B_2(\tau)\right\}, \tag{43}$$

which implies that $\lim_{\xi\mapsto\infty}\langle\mathbf{V}(\xi)\rangle=\frac{\mathbf{q}\pi}{(\rho_1+\delta_1)}$.

Finally, we have

$$\langle\mathbf{R}\rangle=\frac{1}{(\chi+\delta_1)}\left\{\zeta\langle\mathbf{I}\rangle+\frac{\mathbf{R}(0)-\mathbf{R}(\xi)}{\xi}+\frac{\sigma_4}{\xi}\int_0^{\xi}\mathbf{R}(\tau)d\,B_4(\tau)\right\}. \tag{44}$$

which leads to $\lim_{\xi\mapsto\infty}\langle\mathbf{R}(\xi)\rangle=0$, which is the required result. □

Numerical scheme of the proposed model via fractal–fractional derivative operators

In what follows, the framework is further extended to F–F derivative operators in the Atangana–Baleanu sense.

Here, we intend to modify the system by employing the Atangana–Baleanu F–F differential operator instead of the conventional differential operator. We will propose a numerical result for the continually improving system (10) using an innovative numerical approach introduced by Atangana and Araz [34] because it is inherently unpredictable and intricate. As a result, we analyse the approach below.

$$\begin{cases}
{}_0^{\mathrm{FFM}}\mathbf{D}_{\xi}^{\varphi,\omega}\mathbf{S}(\xi)=\left((1-\mathbf{q})\pi+\rho_1\mathbf{V}+\chi\mathbf{R}-\delta_1\mathbf{S}-\vartheta\rho_2\mathbf{SI}\right)+\sigma_1G_1(\xi,\mathbf{S})B_1(\xi),\\
{}_0^{\mathrm{FFM}}\mathbf{D}_{\xi}^{\varphi,\omega}\mathbf{V}(\xi)=\left(\mathbf{q}\pi-\gamma\rho_2\vartheta\mathbf{VI}-(\rho_1+\delta_1)\mathbf{V}\right)+\sigma_2G_2(\xi,\mathbf{V})B_2(\xi),\\
{}_0^{\mathrm{FFM}}\mathbf{D}_{\xi}^{\varphi,\omega}\mathbf{I}(\xi)=\left(\vartheta\varsigma\mathbf{SI}+\gamma\vartheta\rho_2\mathbf{VI}-(\delta_1+\delta_2+\zeta)\mathbf{I}\right)+\sigma_3G_3(\xi,\mathbf{I})B_3(\xi),\\
{}_0^{\mathrm{FFM}}\mathbf{D}_{\xi}^{\varphi,\omega}\mathbf{R}(\xi)=\left(\zeta\mathbf{I}-\chi\mathbf{R}-\delta_1\mathbf{R}\right)+\sigma_4G_4(\xi,\mathbf{R})B_4(\xi).
\end{cases} \tag{45}$$

For $t_{n+1}=(n+1)\Delta\xi$, then we transform these mappings by their polynomials as follows:

$$\begin{aligned}
\mathbf{S}_{n+1}&=\mathbf{S}_0+\frac{(1-\varphi)}{\mathbb{ABC}(\varphi)}\omega\xi_{n+1}^{\omega-1}\left[\begin{cases}\mathbf{S}^*\left(\xi_{n+1},\mathbf{S}_{n+1}^{\mathrm{p}},\mathbf{V}_{n+1}^{\mathrm{p}},\mathbf{I}_{n+1}^{\mathrm{p}},\mathbf{R}_{n+1}^{\mathrm{p}}\right)\\+\sigma_1G_1\left(\xi_{n+1},\mathbf{S}_{n+1}^{\mathrm{p}}\right)\left(B_1(\xi_{n+2})-B_1(\xi_{n+1})\right)\end{cases}\right]\\
&+\frac{\varphi\omega}{\mathbb{ABC}(\varphi)\Gamma(\varphi)}\sum_{j=0}^{n-1}\left[\begin{cases}\mathbf{S}^*\left(\xi_{j+1},\mathbf{S}_{j+1},\mathbf{V}_{j+1},\mathbf{I}_{j+1},\mathbf{R}_{j+1}\right)\mathbf{J}_{1,j}^{\varphi,\omega}\\+\frac{\mathbf{S}^*\left(\xi_{j+1},\mathbf{S}_{j+1},\mathbf{V}_{j+1},\mathbf{I}_{j+1},\mathbf{R}_{j+1}\right)-\mathbf{S}^*\left(\xi_j,\mathbf{S}_j,\mathbf{V}_j,\mathbf{I}_j,\mathbf{R}_j\right)}{\hbar}\mathbf{J}_{2,j}^{\varphi,\omega}\\+\left(\frac{\mathbf{S}^*\left(\xi_{j+1},\mathbf{S}_{j+1},\mathbf{V}_{j+1},\mathbf{I}_{j+1},\mathbf{R}_{j+1}\right)-2\mathbf{S}^*\left(\xi_j,\mathbf{S}_j,\mathbf{V}_j,\mathbf{I}_j,\mathbf{R}_j\right)}{\hbar}\right.\\\left.+\frac{\mathbf{S}^*\left(\xi_{j-1},\mathbf{S}_{j-1},\mathbf{V}_{j-1},\mathbf{I}_{j-1},\mathbf{R}_{j-1}\right)}{\hbar}\right)\mathbf{J}_{3,j}^{\varphi,\omega}\end{cases}\right]\\
&+\frac{\varphi\omega}{\mathbb{ABC}(\varphi)\Gamma(\varphi)}\sum_{j=0}^{n-1}\left[\begin{cases}\sigma_1G_1\left(\xi_{j+1},\mathbf{S}_{j+1}\right)\left(B_1(\xi_{j+1})-B_1(\xi_j)\right)\mathbf{J}_{1,j}^{\varphi,\omega}\\+\left\{\begin{array}{l}\sigma_1G_1\left(\xi_{j+1},\mathbf{S}_{j+1}\right)\left(B_1(\xi_{j+1})-B_1(\xi_j)\right)\\-\sigma_1G_1\left(\xi_j,\mathbf{S}_j\right)\left(B_1(\xi_j)-B_1(\xi_{j-1})\right)\end{array}\right\}\mathbf{J}_{2,j}^{\varphi,\omega}\\+\left\{\frac{\sigma_1G_1\left(\xi_{j+1},\mathbf{S}_{j+1}\right)\left(B_1(\xi_{j+1})-B_1(\xi_j)\right)-2\sigma_1G_1\left(\xi_j,\mathbf{S}_j\right)\left(B_1(\xi_j)-B_1(\xi_{j-1})\right)}{\hbar}\right.\\\left.-\frac{\sigma_1G_1\left(\xi_{j-1},\mathbf{S}_{j-1}\right)\left(B_1(\xi_{j-1})-B_1(\xi_{j-2})\right)}{\hbar}\right\}\mathbf{J}_{3,j}^{\varphi,\omega}\end{cases}\right]\\
&+\frac{\varphi\omega}{\mathbb{ABC}(\varphi)\Gamma(\varphi)}\left[\begin{cases}\mathbf{S}^*\left(\xi_{n+1},\mathbf{S}_{n+1}^{\mathrm{p}},\mathbf{V}_{n+1}^{\mathrm{p}},\mathbf{I}_{n+1}^{\mathrm{p}},\mathbf{R}_{n+1}^{\mathrm{p}}\right)\mathbf{J}_{1,n}^{\varphi,\omega}\\+\mathbf{S}^*\left(\xi_{n+1},\mathbf{S}_{n+1}^{\mathrm{p}},\mathbf{V}_{n+1}^{\mathrm{p}},\mathbf{I}_{n+1}^{\mathrm{p}},\mathbf{R}_{n+1}^{\mathrm{p}}\right)\mathbf{J}_{2,n}^{\varphi,\omega}\\-\mathbf{S}^*\left(\xi_n,\mathbf{S}_n,\mathbf{V}_n,\mathbf{I}_n,\mathbf{R}_n\right)\mathbf{J}_{2,n}^{\varphi,\omega}\\+\left\{\frac{\mathbf{S}^*\left(\xi_{n+1},\mathbf{S}_{n+1}^{\mathrm{p}},\mathbf{V}_{n+1}^{\mathrm{p}},\mathbf{I}_{n+1}^{\mathrm{p}},\mathbf{R}_{n+1}^{\mathrm{p}}\right)-2\mathbf{S}^*\left(\xi_n,\mathbf{S}_n,\mathbf{V}_n,\mathbf{I}_n,\mathbf{R}_n\right)}{2\hbar}\right\}\mathbf{J}_{3,n}^{\varphi,\omega}\\+\frac{\mathbf{S}^*\left(\xi_{n-1},\mathbf{S}_{n-1},\mathbf{V}_{n-1},\mathbf{I}_{n-1},\mathbf{R}_{n-1}\right)}{2\hbar^2}\mathbf{J}_{3,n}^{\varphi,\omega}\\+\sigma_1G_1\left(\xi_{n+1},\mathbf{S}_{n+1}^{\mathrm{p}}\right)\left(B_1(\xi_{n+1})-B_1(\xi_n)\right)\mathbf{J}_{1,n}^{\varphi,\omega}\\+\sigma_1G_1\left(\xi_{n+1},\mathbf{S}_{n+1}^{\mathrm{p}}\right)\left(B_1(\xi_{n+1})-B_1(\xi_n)\right)\mathbf{J}_{2,n}^{\varphi,\omega}\\-\sigma_1G_1\left(\xi_n,\mathbf{S}_n^{\mathrm{p}}\right)\left(B_1(\xi_n)-B_1(\xi_{n-1})\right)\mathbf{J}_{2,n}^{\varphi,\omega}\\+\frac{\sigma_1G_1\left(\xi_{n+1},\mathbf{S}_{n+1}^{\mathrm{p}}\right)\left(B_1(\xi_{n+1})-B_1(\xi_n)\right)}{2\hbar}\mathbf{J}_{3,n}^{\varphi,\omega}\\-2\frac{\sigma_1G_1\left(\xi_n,\mathbf{S}_n^{\mathrm{p}}\right)\left(B_1(\xi_n)-B_1(\xi_{n-1})\right)}{2\hbar}\mathbf{J}_{3,n}^{\varphi,\omega}\\+\frac{\sigma_1G_1\left(\xi_{n-1},\mathbf{S}_{n-1}^{\mathrm{p}}\right)\left(B_1(\xi_{n-2})-B_1(\xi_{n-2})\right)}{2\hbar}\mathbf{J}_{3,n}^{\varphi,\omega}\end{cases}\right],
\end{aligned} \tag{46}$$

$$\begin{aligned}
\mathbf{V}_{n+1}&=\mathbf{V}_0+\frac{(1-\varphi)}{\mathbb{ABC}(\varphi)}\omega\xi_{n+1}^{\omega-1}\left[\begin{cases}\mathbf{V}^*\left(\xi_{n+1},\mathbf{V}_{n+1}^{\mathrm{p}},\mathbf{I}_{n+1}^{\mathrm{p}}\right)\\+\sigma_2G_2\left(\xi_{n+1},\mathbf{V}_{n+1}^{\mathrm{p}}\right)\left(B_2(\xi_{n+2})-B_2(\xi_{n+1})\right)\end{cases}\right]\\
&+\frac{\varphi\omega}{\mathbb{ABC}(\varphi)\Gamma(\varphi)}\sum_{j=0}^{n-1}\left[\begin{cases}\mathbf{V}^*\left(\xi_{j+1},\mathbf{V}_{j+1},\mathbf{I}_{j+1}\right)\mathbf{J}_{1,j}^{\varphi,\omega}\\+\frac{\mathbf{V}^*\left(\xi_{j+1},\mathbf{V}_{j+1},\mathbf{I}_{j+1}\right)-\mathbf{V}^*\left(\xi_j,\mathbf{V}_j,\mathbf{I}_j\right)}{\hbar}\mathbf{J}_{2,j}^{\varphi,\omega}\\+\frac{\mathbf{V}^*\left(\xi_{j+1},\mathbf{V}_{j+1},\mathbf{I}_{j+1}\right)-2\mathbf{V}^*\left(\xi_j,\mathbf{V}_j,\mathbf{I}_j\right)+\mathbf{V}^*\left(\xi_{j-1},\mathbf{V}_{j-1},\mathbf{I}_{j-1}\right)}{\hbar}\mathbf{J}_{3,j}^{\varphi,\omega}\end{cases}\right]\\
&+\frac{\varphi\omega}{\mathbb{ABC}(\varphi)\Gamma(\varphi)}\sum_{j=0}^{n-1}\left[\begin{cases}\sigma_2G_2\left(\xi_{j+1},\mathbf{V}_{j+1}\right)\left(B_2(\xi_{j+1})-B_2(\xi_j)\right)\mathbf{J}_{1,j}^{\varphi,\omega}\\+\left\{\begin{array}{l}\sigma_2G_2\left(\xi_{j+1},\mathbf{V}_{j+1}\right)\left(B_2(\xi_{j+1})-B_2(\xi_j)\right)\\-\sigma_2G_2\left(\xi_j,\mathbf{V}_j\right)\left(B_2(\xi_j)-B_2(\xi_{j-1})\right)\end{array}\right\}\mathbf{J}_{2,j}^{\varphi,\omega}\\+\left\{\frac{\sigma_2G_2\left(\xi_{j+1},\mathbf{V}_{j+1}\right)\left(B_2(\xi_{j+1})-B_2(\xi_j)\right)-2\sigma_2G_2\left(\xi_j,\mathbf{V}_j\right)\left(B_2(\xi_j)-B_2(\xi_{j-1})\right)}{\hbar}\right.\\\left.-\frac{\sigma_2G_2\left(\xi_{j-1},\mathbf{V}_{j-1}\right)\left(B_2(\xi_{j-1})-B_2(\xi_{j-2})\right)}{\hbar}\right\}\mathbf{J}_{3,j}^{\varphi,\omega}\end{cases}\right]\\
&+\frac{\varphi\omega}{\mathbb{ABC}(\varphi)\Gamma(\varphi)}\left[\begin{cases}\mathbf{V}^*\left(\xi_{n+1},\mathbf{V}_{n+1}^{\mathrm{p}},\mathbf{I}_{n+1}^{\mathrm{p}}\right)\mathbf{J}_{1,n}^{\varphi,\omega}\\+\mathbf{V}^*\left(\xi_{n+1},\mathbf{V}_{n+1}^{\mathrm{p}},\mathbf{I}_{n+1}^{\mathrm{p}}\right)\mathbf{J}_{2,n}^{\varphi,\omega}\\-\mathbf{V}^*\left(\xi_n,\mathbf{V}_n,\mathbf{I}_n\right)\mathbf{J}_{2,n}^{\varphi,\omega}\\+\left\{\frac{\mathbf{V}^*\left(\xi_{n+1},\mathbf{V}_{n+1}^{\mathrm{p}},\mathbf{I}_{n+1}^{\mathrm{p}}\right)-2\mathbf{V}^*\left(\xi_n,\mathbf{V}_n,\mathbf{I}_n\right)}{2\hbar}\right\}\mathbf{J}_{3,n}^{\varphi,\omega}\\+\frac{\mathbf{V}^*\left(\xi_{n-1},\mathbf{V}_{n-1},\mathbf{I}_{n-1}\right)}{2\hbar^2}\mathbf{J}_{3,n}^{\varphi,\omega}\\+\sigma_2G_2\left(\xi_{n+1},\mathbf{V}_{n+1}^{\mathrm{p}}\right)\left(B_2(\xi_{n+1})-B_2(\xi_n)\right)\mathbf{J}_{1,n}^{\varphi,\omega}\\+\sigma_2G_2\left(\xi_{n+1},\mathbf{V}_{n+1}^{\mathrm{p}}\right)\left(B_2(\xi_{n+1})-B_2(\xi_n)\right)\mathbf{J}_{2,n}^{\varphi,\omega}\\-\sigma_2G_2\left(\xi_n,\mathbf{V}_n^{\mathrm{p}}\right)\left(B_2(\xi_n)-B_2(\xi_{n-1})\right)\mathbf{J}_{2,n}^{\varphi,\omega}\\+\frac{\sigma_2G_2\left(\xi_{n+1},\mathbf{V}_{n+1}^{\mathrm{p}}\right)\left(B_2(\xi_{n+1})-B_2(\xi_n)\right)}{2\hbar}\mathbf{J}_{3,n}^{\varphi,\omega}\\-2\frac{\sigma_2G_2\left(\xi_n,\mathbf{V}_n^{\mathrm{p}}\right)\left(B_2(\xi_n)-B_2(\xi_{n-1})\right)}{2\hbar}\mathbf{J}_{3,n}^{\varphi,\omega}\\+\frac{\sigma_2G_2\left(\xi_{n-1},\mathbf{V}_{n-1}^{\mathrm{p}}\right)\left(B_2(\xi_{n-2})-B_2(\xi_{n-2})\right)}{2\hbar}\mathbf{J}_{3,n}^{\varphi,\omega}\end{cases}\right],
\end{aligned} \tag{47}$$

$$\begin{aligned}
\mathbf{I}_{n+1}&=\mathbf{I}_0+\frac{(1-\varphi)}{\mathbb{ABC}(\varphi)}\omega\xi_{n+1}^{\omega-1}\left[\begin{cases}\mathbf{I}^*\left(\xi_{n+1},\mathbf{S}_{n+1}^{\mathrm{p}},\mathbf{V}_{n+1}^{\mathrm{p}},\mathbf{I}_{n+1}^{\mathrm{p}}\right)\\+\sigma_3G_4\left(\xi_{n+1},\mathbf{I}_{n+1}^{\mathrm{p}}\right)\left(B_3(\xi_{n+2})-B_3(\xi_{n+1})\right)\end{cases}\right]\\
&+\frac{\varphi\omega}{\mathbb{ABC}(\varphi)\Gamma(\varphi)}\sum_{j=0}^{n-1}\left[\begin{cases}\mathbf{I}^*\left(\xi_{j+1},\mathbf{S}_{j+1},\mathbf{V}_{j+1},\mathbf{I}_{j+1}\right)\mathbf{J}_{1,j}^{\varphi,\omega}\\+\frac{\mathbf{I}^*\left(\xi_{j+1},\mathbf{S}_{j+1},\mathbf{V}_{j+1},\mathbf{I}_{j+1}\right)-\mathbf{I}^*\left(\xi_j,\mathbf{S}_j,\mathbf{V}_j,\mathbf{I}_j\right)}{\hbar}\mathbf{J}_{2,j}^{\varphi,\omega}\\+\frac{\mathbf{I}^*\left(\xi_{j+1},\mathbf{S}_{j+1},\mathbf{V}_{j+1},\mathbf{I}_{j+1}\right)-2\mathbf{I}^*\left(\xi_j,\mathbf{S}_j,\mathbf{V}_j,\mathbf{I}_j\right)+\mathbf{I}^*\left(\xi_{j-1},\mathbf{S}_{j-1},\mathbf{V}_{j-1},\mathbf{I}_{j-1}\right)}{\hbar}\mathbf{J}_{3,j}^{\varphi,\omega}\end{cases}\right]
\end{aligned}$$

$$+\frac{\varphi\omega}{\mathbb{ABC}(\varphi)\Gamma(\varphi)}\sum_{j=0}^{n-1}\left[\begin{cases}\sigma_3 G_3\left(\xi_{j+1},\mathbf{I}_{j+1}\right)\left(B_3(\xi_{j+1})-B_3(\xi_j)\right)\mathbf{J}_{1,j}^{\varphi,\omega}\\ +\left\{\begin{array}{l}\sigma_3 G_3\left(\xi_{j+1},\mathbf{I}_{j+1}\right)\left(B_3(\xi_{j+1})-B_3(\xi_j)\right)\\ -\sigma_3 G_3\left(\xi_j,\mathbf{I}_j\right)\left(B_3(\xi_j)-B_3(\xi_{j-1})\right)\end{array}\right\}\mathbf{J}_{2,j}^{\varphi,\omega}\\ +\left\{\begin{array}{l}\frac{\sigma_3 G_3\left(\xi_{j+1},\mathbf{I}_{j+1}\right)\left(B_3(\xi_{j+1})-B_3(\xi_j)\right)-2\sigma_3 G_3\left(\xi_j,\mathbf{I}_j\right)\left(B_3(\xi_j)-B_3(\xi_{j-1})\right)}{\hbar}\\ -\frac{\sigma_3 G_3\left(\xi_{j-1},\mathbf{I}_{j-1}\right)\left(B_3(\xi_{j-1})-B_3(\xi_{j-2})\right)}{\hbar}\end{array}\right\}\mathbf{J}_{3,j}^{\varphi,\omega}\end{cases}\right]$$

$$+\frac{\varphi\omega}{\mathbb{ABC}(\varphi)\Gamma(\varphi)}\left[\begin{cases}\mathbf{I}^*\left(\xi_{n+1},\mathbf{S}_{n+1}^{\mathrm{p}},\mathbf{V}_{n+1}^{\mathrm{p}},\mathbf{I}_{n+1}^{\mathrm{p}}\right)\mathbf{J}_{1,n}^{\varphi,\omega}\\ +\mathbf{I}^*\left(\xi_{n+1},\mathbf{S}_{n+1}^{\mathrm{p}},\mathbf{V}_{n+1}^{\mathrm{p}},\mathbf{I}_{n+1}^{\mathrm{p}}\right)\mathbf{J}_{2,n}^{\varphi,\omega}\\ -\mathbf{I}^*\left(\xi_n,\mathbf{S}_n,\mathbf{V}_n,\mathbf{I}_n\right)\mathbf{J}_{2,n}^{\varphi,\omega}\\ +\left\{\frac{\mathbf{I}^*\left(\xi_{n+1},\mathbf{S}_{n+1}^{\mathrm{p}},\mathbf{V}_{n+1}^{\mathrm{p}},\mathbf{I}_{n+1}^{\mathrm{p}}\right)-2\mathbf{I}^*\left(\xi_n,\mathbf{S}_n,\mathbf{V}_n,\mathbf{I}_n\right)}{2\hbar}\right\}\mathbf{J}_{3,n}^{\varphi,\omega}\\ +\frac{\mathbf{I}^*\left(\xi_{n-1},\mathbf{S}_{n-1},\mathbf{V}_{n-1},\mathbf{I}_{n-1}\right)}{2\hbar^2}\mathbf{J}_{3,n}^{\varphi,\omega}\\ +\sigma_3 G_3\left(\xi_{n+1},\mathbf{I}_{n+1}^{\mathrm{p}}\right)\left(B_3(\xi_{n+1})-B_3(\xi_n)\right)\mathbf{J}_{1,n}^{\varphi,\omega}\\ +\sigma_3 G_3\left(\xi_{n+1},\mathbf{I}_{n+1}^{\mathrm{p}}\right)\left(B_3(\xi_{n+1})-B_3(\xi_n)\right)\mathbf{J}_{2,n}^{\varphi,\omega}\\ -\sigma_3 G_3\left(\xi_n,\mathbf{I}_n^{\mathrm{p}}\right)\left(B_3(\xi_n)-B_3(\xi_{n-1})\right)\mathbf{J}_{2,n}^{\varphi,\omega}\\ +\frac{\sigma_3 G_3\left(\xi_{n+1},\mathbf{I}_{n+1}^{\mathrm{p}}\right)\left(B_3(\xi_{n+1})-B_3(\xi_n)\right)}{2\hbar}\mathbf{J}_{3,n}^{\varphi,\omega}\\ -2\frac{\sigma_3 G_3\left(\xi_n,\mathbf{I}_n^{\mathrm{p}}\right)\left(B_3(\xi_n)-B_3(\xi_{n-1})\right)}{2\hbar}\mathbf{J}_{3,n}^{\varphi,\omega}\\ +\frac{\sigma_3 G_3\left(\xi_{n-1},\mathbf{I}_{n-1}^{\mathrm{p}}\right)\left(B_3(\xi_{n-2})-B_3(\xi_{n-2})\right)}{2\hbar}\mathbf{J}_{3,n}^{\varphi,\omega}\end{cases}\right],\tag{48}$$

$$\mathbf{R}_{n+1}=\mathbf{R}_0+\frac{(1-\varphi)}{\mathbb{ABC}(\varphi)}\omega\xi_{n+1}^{\omega-1}\left[\begin{cases}\mathbf{R}^*\left(\xi_{n+1},\mathbf{I}_{n+1}^{\mathrm{p}},\mathbf{R}_{n+1}^{\mathrm{p}}\right)\\ +\sigma_4 G_4\left(\xi_{n+1},\mathbf{R}_{n+1}^{\mathrm{p}}\right)\left(B_4(\xi_{n+2})-B_4(\xi_{n+1})\right)\end{cases}\right]$$

$$+\frac{\varphi\omega}{\mathbb{ABC}(\varphi)\Gamma(\varphi)}\sum_{j=0}^{n-1}\left[\begin{cases}\mathbf{R}^*\left(\xi_{j+1},\mathbf{I}_{j+1},\mathbf{R}_{j+1}\right)\mathbf{J}_{1,j}^{\varphi,\omega}\\ +\frac{\mathbf{R}^*\left(\xi_{j+1},\mathbf{I}_{j+1},\mathbf{R}_{j+1}\right)-\mathbf{R}^*\left(\xi_j,\mathbf{I}_j,\mathbf{R}_j\right)}{\hbar}\mathbf{J}_{2,j}^{\varphi,\omega}\\ +\frac{\mathbf{R}^*\left(\xi_{j+1},\mathbf{I}_{j+1},\mathbf{R}_{j+1}\right)-2\mathbf{I}^*\left(\xi_j,\mathbf{I}_j,\mathbf{R}_j\right)+\mathbf{R}^*\left(\xi_{j-1},\mathbf{I}_{j-1},\mathbf{R}_{j-1}\right)}{\hbar}\mathbf{J}_{3,j}^{\varphi,\omega}\end{cases}\right]$$

$$+\frac{\varphi\omega}{\mathbb{ABC}(\varphi)\Gamma(\varphi)}\sum_{j=0}^{n-1}\left[\begin{cases}\sigma_4 G_4\left(\xi_{j+1},\mathbf{R}_{j+1}\right)\left(B_4(\xi_{j+1})-B_4(\xi_j)\right)\mathbf{J}_{1,j}^{\varphi,\omega}\\ +\left\{\begin{array}{l}\sigma_4 G_4\left(\xi_{j+1},\mathbf{R}_{j+1}\right)\left(B_4(\xi_{j+1})-B_4(\xi_j)\right)\\ -\sigma_4 G_4\left(\xi_j,\mathbf{R}_j\right)\left(B_4(\xi_j)-B_4(\xi_{j-1})\right)\end{array}\right\}\mathbf{J}_{2,j}^{\varphi,\omega}\\ +\left\{\begin{array}{l}\frac{\sigma_4 G_4\left(\xi_{j+1},\mathbf{I}_{j+1}\right)\left(B_4(\xi_{j+1})-B_4(\xi_j)\right)-2\sigma_4 G_4\left(\xi_j,\mathbf{R}_j\right)\left(B_4(\xi_j)-B_4(\xi_{j-1})\right)}{\hbar}\\ -\frac{\sigma_4 G_4\left(\xi_{j-1},\mathbf{R}_{j-1}\right)\left(B_4(\xi_{j-1})-B_4(\xi_{j-2})\right)}{\hbar}\end{array}\right\}\mathbf{J}_{3,j}^{\varphi,\omega}\end{cases}\right]$$

$$+\frac{\varphi\omega}{\mathbb{ABC}(\varphi)\Gamma(\varphi)}\left[\begin{cases}\mathbf{R}^*\left(\xi_{n+1},\mathbf{I}_{n+1}^{\mathrm{p}},\mathbf{R}_{n+1}^{\mathrm{p}}\right)\mathbf{J}_{1,n}^{\varphi,\omega}\\ +\mathbf{R}^*\left(\xi_{n+1},\mathbf{I}_{n+1}^{\mathrm{p}},\mathbf{R}_{n+1}^{\mathrm{p}}\right)\mathbf{J}_{2,n}^{\varphi,\omega}\\ -\mathbf{R}^*\left(\xi_n,\mathbf{I}_n,\mathbf{R}_n\right)\mathbf{J}_{2,n}^{\varphi,\omega}\\ +\left\{\frac{\mathbf{R}^*\left(\xi_{n+1},\mathbf{I}_{n+1}^{\mathrm{p}},\mathbf{R}_{n+1}^{\mathrm{p}}\right)-2\mathbf{R}^*\left(\xi_n,\mathbf{I}_n,\mathbf{R}_n\right)}{2\hbar}\right\}\mathbf{J}_{3,n}^{\varphi,\omega}\\ +\frac{\mathbf{R}^*\left(\xi_{n-1},\mathbf{I}_{n-1},\mathbf{R}_{n-1}\right)}{2\hbar^2}\mathbf{J}_{3,n}^{\varphi,\omega}\\ +\sigma_4 G_4\left(\xi_{n+1},\mathbf{R}_{n+1}^{\mathrm{p}}\right)\left(B_4(\xi_{n+1})-B_4(\xi_n)\right)\mathbf{J}_{1,n}^{\varphi,\omega}\\ +\sigma_4 G_4\left(\xi_{n+1},\mathbf{R}_{n+1}^{\mathrm{p}}\right)\left(B_4(\xi_{n+1})-B_4(\xi_n)\right)\mathbf{J}_{2,n}^{\varphi,\omega}\\ -\sigma_4 G_4\left(\xi_n,\mathbf{R}_n^{\mathrm{p}}\right)\left(B_4(\xi_n)-B_4(\xi_{n-1})\right)\mathbf{J}_{2,n}^{\varphi,\omega}\\ +\frac{\sigma_4 G_4\left(\xi_{n+1},\mathbf{R}_{n+1}^{\mathrm{p}}\right)\left(B_4(\xi_{n+1})-B_4(\xi_n)\right)}{2\hbar}\mathbf{J}_{3,n}^{\varphi,\omega}\\ -2\frac{\sigma_4 G_4\left(\xi_n,\mathbf{R}_n^{\mathrm{p}}\right)\left(B_4(\xi_n)-B_4(\xi_{n-1})\right)}{2\hbar}\mathbf{J}_{3,n}^{\varphi,\omega}\\ +\frac{\sigma_4 G_4\left(\xi_{n-1},\mathbf{R}_{n-1}^{\mathrm{p}}\right)\left(B_4(\xi_{n-2})-B_4(\xi_{n-2})\right)}{2\hbar}\mathbf{J}_{3,n}^{\varphi,\omega}\end{cases}\right],\tag{49}$$

where

$$\mathbf{S}_{n+1}^{\mathrm{p}}=\mathbf{S}_0+\frac{1-\varphi}{\mathbb{ABC}(\varphi)}\omega\xi_{n+1}^{\omega-1}\left[\begin{cases}\mathbf{S}^*\left(\xi_n,\mathbf{S}_n,\mathbf{V}_n,\mathbf{I}_n,\mathbf{R}_n\right)\\ +\omega\sigma_1 G_1\left(\xi_n,\mathbf{S}_n\right)\left(B_1(\xi_n)-B_1(\xi_{n-1})\right)\end{cases}\right]$$

$$+\frac{\varphi\omega}{\mathbb{ABC}(\varphi)\Gamma(\varphi)}\sum_{j=0}^{n}\left[\begin{cases}\mathbf{S}^*\left(\xi_j,\mathbf{S}_j,\mathbf{V}_j,\mathbf{I}_j,\mathbf{R}_j\right)\mathbf{J}_{1,j}^{\varphi,\omega}\\ +\sigma_1 G_1\left(\xi_j,\mathbf{S}_j\right)\left(B_1(\xi_j)-B_1(\xi_{j-1})\right)\mathbf{J}_{1,j}^{\varphi,\omega}\end{cases}\right],$$

$$\mathbf{V}_{n+1}^{\mathrm{p}}=\mathbf{V}_0+\frac{1-\varphi}{\mathbb{ABC}(\varphi)}\omega\xi_{n+1}^{\omega-1}\left[\begin{cases}\mathbf{V}^*\left(\xi_n,\mathbf{V}_n,\mathbf{I}_n\right)\\ +\omega\sigma_2 G_2\left(\xi_n,\mathbf{V}_n\right)\left(B_2(\xi_n)-B_2(\xi_{n-1})\right)\end{cases}\right]$$

$$+\frac{\varphi\omega}{\mathbb{ABC}(\varphi)\Gamma(\varphi)}\sum_{j=0}^{n}\left[\begin{cases}\mathbf{V}^*\left(\xi_j,\mathbf{V}_j,\mathbf{I}_j\right)\mathbf{J}_{1,j}^{\varphi,\omega}\\ +\sigma_2 G_2\left(\xi_j,\mathbf{V}_j\right)\left(B_2(\xi_j)-B_2(\xi_{j-1})\right)\mathbf{J}_{1,j}^{\varphi,\omega}\end{cases}\right],$$

$$\mathbf{I}_{n+1}^{\mathrm{p}}=\mathbf{I}_0+\frac{1-\varphi}{\mathbb{ABC}(\varphi)}\omega\xi_{n+1}^{\omega-1}\left[\begin{cases}\mathbf{I}^*\left(\xi_n,\mathbf{S}_n,\mathbf{V}_n,\mathbf{I}_n\right)\\ +\omega\sigma_3 G_3\left(\xi_n,\mathbf{I}_n\right)\left(B_3(\xi_n)-B_3(\xi_{n-1})\right)\end{cases}\right]$$

$$+\frac{\varphi\omega}{\mathbb{ABC}(\varphi)\Gamma(\varphi)}\sum_{j=0}^{n}\left[\begin{cases}\mathbf{I}^*\left(\xi_j,\mathbf{S}_j,\mathbf{V}_j,\mathbf{I}_j\right)\mathbf{J}_{1,j}^{\varphi,\omega}\\ +\sigma_3 G_3\left(\xi_j,\mathbf{I}_j\right)\left(B_3(\xi_j)-B_3(\xi_{j-1})\right)\mathbf{J}_{1,j}^{\varphi,\omega}\end{cases}\right],$$

$$\mathbf{R}_{n+1}^{\mathrm{p}}=\mathbf{R}_0+\frac{1-\varphi}{\mathbb{ABC}(\varphi)}\omega\xi_{n+1}^{\omega-1}\left[\begin{cases}\mathbf{R}^*\left(\xi_n,\mathbf{I}_n,\mathbf{R}_n\right)\\ +\omega\sigma_4 G_4\left(\xi_n,\mathbf{R}_n\right)\left(B_4(\xi_n)-B_4(\xi_{n-1})\right)\end{cases}\right]$$

$$+\frac{\varphi\omega}{\mathbb{ABC}(\varphi)\Gamma(\varphi)}\sum_{j=0}^{n}\left[\begin{cases}\mathbf{R}^*\left(\xi_j,\mathbf{I}_j,\mathbf{R}_j\right)\mathbf{J}_{1,j}^{\varphi,\omega}\\ +\sigma_4 G_4\left(\xi_j,\mathbf{R}_j\right)\left(B_4(\xi_j)-B_4(\xi_{j-1})\right)\mathbf{J}_{1,j}^{\varphi,\omega}\end{cases}\right].\tag{50}$$

where

$$\mathbf{J}_{1,j}^{\varphi,\omega}=\frac{((n+1)\hbar)^{\varphi-1}}{\omega}\left[\begin{cases}((j+1)\hbar)^{\omega}\,{}_2\mathcal{F}_1\left(\left[\omega,1-\varphi\right],\left[1+\omega\right],\frac{j+1}{n+1}\right)\\ -(j\hbar)^{\omega}\,{}_2\mathcal{F}_1\left(\left[\omega,1-\varphi\right],\left[1+\omega\right],\frac{j}{n}\right)\end{cases}\right],$$

$$\mathbf{J}_{2,j}^{\varphi,\omega}=\frac{((n+1)\hbar)^{\varphi-1}}{\omega(\omega+1)}$$

$$\times\left[\begin{cases}\omega((j+1)\hbar)^{\omega+1}\,{}_2\mathcal{F}_1\left(\left[1+\omega,1-\varphi\right],\left[2+\omega\right],\frac{j+1}{n+1}\right)\\ -(1+\omega)((j+1)\hbar)^{\omega+1}\,{}_2\mathcal{F}_1\left(\left[\omega,1-\varphi\right],\left[1+\omega\right],\frac{j+1}{n}\right)\\ -\omega((j)\hbar)^{\omega+1}\,{}_2\mathcal{F}_1\left(\left[1+\omega,1-\varphi\right],\left[2+\omega\right],\frac{j}{n+1}\right)\\ +\hbar((j)\hbar)^{\omega}(1+\omega)(1+j)\,{}_2\mathcal{F}_1\left(\left[\omega,1-\varphi\right],\left[1+\omega\right],\frac{j}{n}\right)\end{cases}\right],$$

$$\mathbf{J}_{3,j}^{\varphi,\omega}=\frac{((j+1)\hbar)^{\varphi-1}}{\omega(\omega+1)(\omega+2)}$$

$$\times\left[\begin{cases}\omega(\omega+1)((j+1)\hbar)^{\omega+2}\,{}_2\mathcal{F}_1\left(\left[2+\omega,1-\varphi\right],\left[3+\omega\right],\frac{j+1}{n+1}\right)\\ -2\omega(\omega+2)\left(j+\frac{1}{2}\right)\hbar((j+1)\hbar)^{\omega+1}\,{}_2\mathcal{F}_1\left(\left[1+\omega,1-\varphi\right],\left[2+\omega\right],\frac{j+1}{n+1}\right)\\ +j\hbar(\omega+1)(\omega+2)((j+1)\hbar)^{\omega+1}\,{}_2\mathcal{F}_1\left(\left[\omega,1-\varphi\right],\left[1+\omega\right],\frac{j+1}{n}\right)\\ +2\omega(\omega+2)\left(j+\frac{1}{2}\right)\hbar((\hbar j))^{\omega+1}\,{}_2\mathcal{F}_1\left(\left[1+\omega,1-\varphi\right],\left[2+\omega\right],\frac{j}{n+1}\right)\\ -\omega(\omega+1)(j\hbar)^{\omega+2}\,{}_2\mathcal{F}_1\left(\left[2+\omega,1-\varphi\right],\left[3+\omega\right],\frac{j}{n}\right)\\ -\hbar(\omega+1)(\omega+2)(j+1)(j\hbar)^{\omega+1}\,{}_2\mathcal{F}_1\left(\left[\omega,1-\varphi\right],\left[1+\omega\right],\frac{j}{n+1}\right)\end{cases}\right].$$

Results and discussion

In this section, we provide and examine certain modelling outcomes for the mechanisms of tuberculosis transmission as described by model (10) via the fractal–fractional derivative in the Atangana–Baleanu sense. Atangana and Araz [34] technique is used to numerically solve stochastic differential equations, and numerical simulations are provided to evaluate our analytical findings. For this purpose, the system's components $\mathbf{q}$, ρ_2, r_1, and ϑ, whose attributes are shown in Table 1, were used. We change the settings of these characteristics to see how they affect the simulations.

The stochastic graphs in Figs. 4 and 5 depict the unpredictability of the population of individuals within each cohort using the F–F derivative in the Atangana–Baleanu sense, with decreases in fractional-order φ while maintaining fractal-dimension to be 1. In essence, this is how meaningful occurrences behave, and the behaviour revealed in the randomized graphs is unsurprising given that stochastic models better capture specific environments than deterministic techniques [14]. These statistics also show that the proportion of contaminated individuals continues to decrease over time, with no ebbs and flows in the determinism scenario and several fluctuations in the randomized situation.

Furthermore, by considering the F–F derivative operator in the context of the Atangana–Baleanu sense, the numerical findings obtained by adjusting the value of ϑ while maintaining the remaining process components are shown in Figs. 6 and 7. Due to the unpredictability behaviour, the outcomes from the stochastic approach, illustrated in Figs. 6 and 7, are likewise rising, keeping their crisscrossing structure

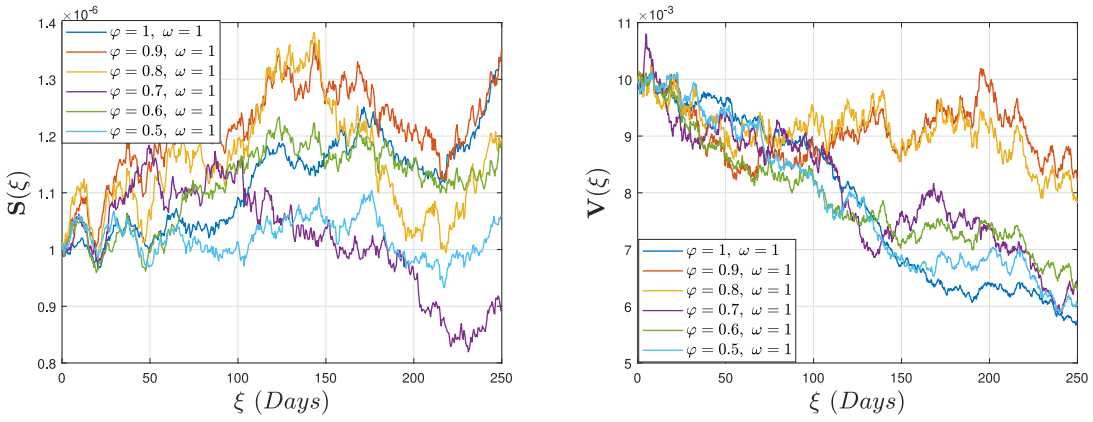

Fig. 4. Trajectories for the susceptible $\mathbf{S}(\xi)$ and vaccinated $\mathbf{V}(\xi)$ when the white noise values $\sigma_1 = 0.5,\ \sigma_2 = 0.6,\ \sigma_3 = 0.8,\ \sigma_4 = 0.85$ have a significant decrease in φ while considering $\omega = 1$.

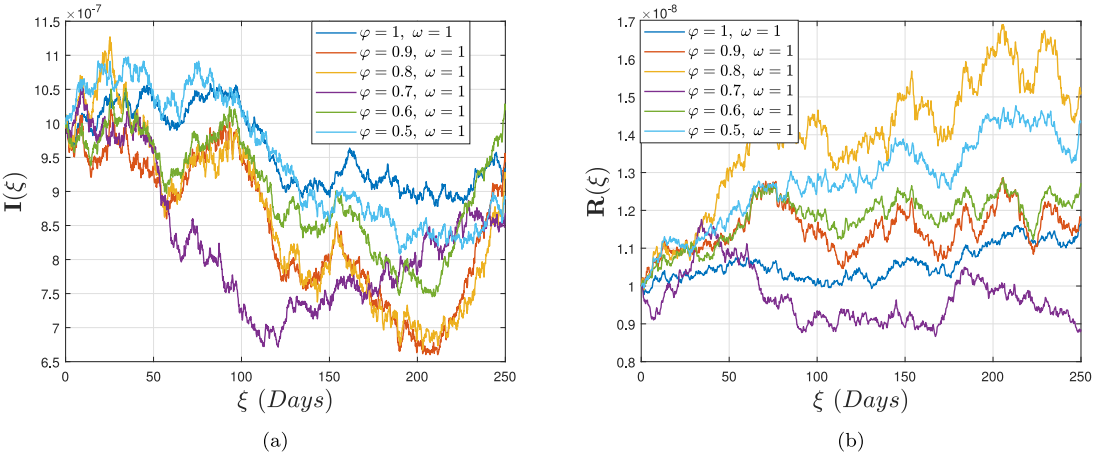

Fig. 5. Trajectories for the Infected $\mathbf{R}(\xi)$ and restored $\mathbf{R}(\xi)$ when the white noise values $\sigma_1 = 0.5,\ \sigma_2 = 0.6,\ \sigma_3 = 0.8,\ \sigma_4 = 0.85$ have a significant decrease in φ while considering $\omega = 1$.

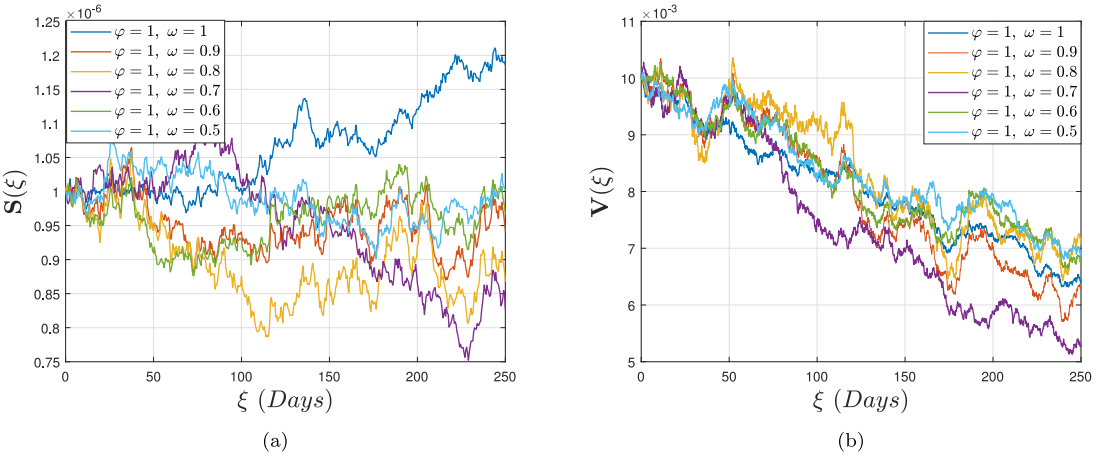

Fig. 6. Trajectories for the susceptible $\mathbf{S}(\xi)$ and vaccinated $\mathbf{V}(\xi)$ when the white noise values $\sigma_1 = 0.9,\ \sigma_2 = 1.0,\ \sigma_3 = 1.1,\ \sigma_4 = 1.3$ have a significant decrease in ω while considering $\varphi = 1$.

(effectively approximating the clear illustration) whilst keeping φ to be fixed and ω to be decreased. This significant difference indicates that the infection decreased when the contact rate ϑ was increased from $\vartheta = 0.07$ to $\vartheta = 0.1$. Also, the general result is that when the value of ϑ significantly increased, the number of affected individuals begins to rise dramatically. As a result, we can deduce that, especially when various characteristics stay unchanged, the infection rate rises in the population as the randomness of interaction rate rises.

Figs. 8 and 9 show the numerical results of varying the level of component **q** (inoculation rate) while holding the other factors constant

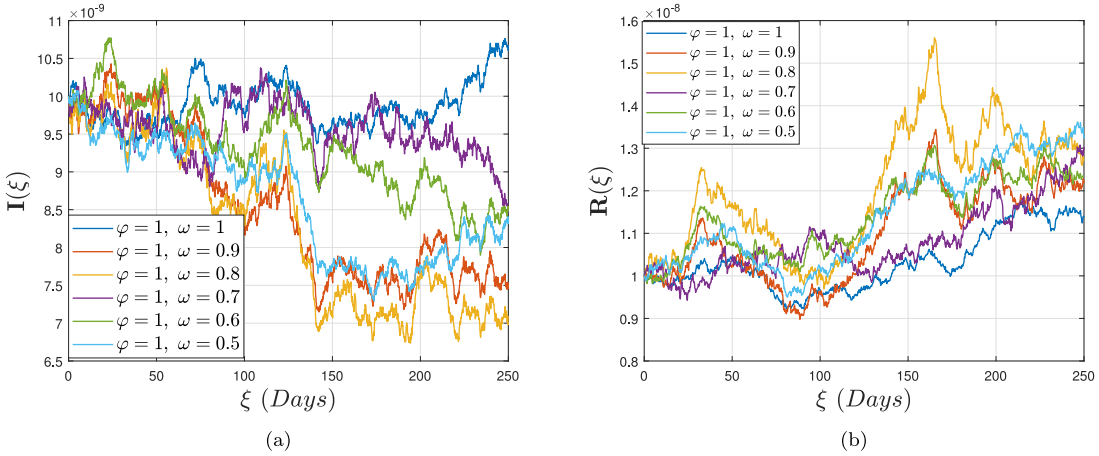

Fig. 7. Trajectories for the infected $\mathbf{I}(\xi)$ and restored $\mathbf{R}(\xi)$ when the white noise values $\sigma_1 = 0.9,\ \sigma_2 = 1.0,\ \sigma_3 = 1.1,\ \sigma_4 = 1.3$ have a significant decrease in ω while considering $\varphi = 1$.

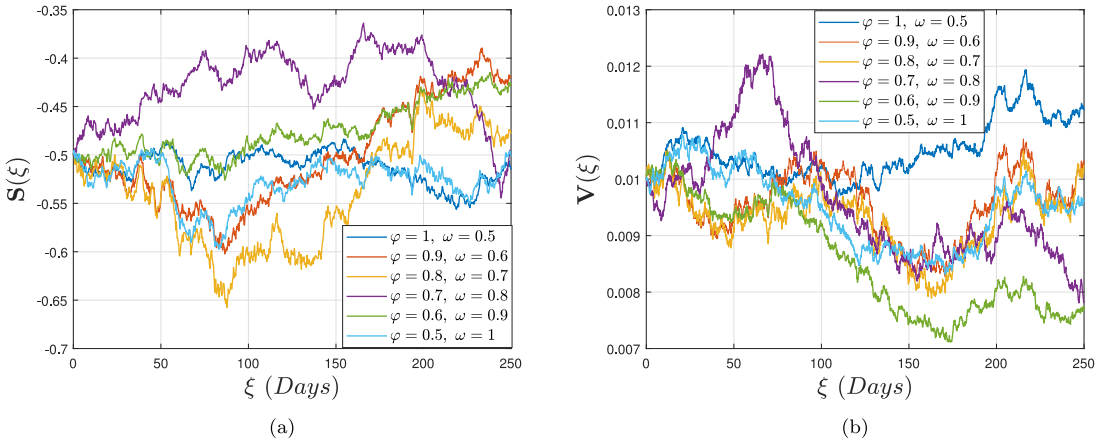

Fig. 8. Trajectories for the susceptible $\mathbf{S}(\xi)$ and vaccinated $\mathbf{V}(\xi)$ when the white noise values $\sigma_1 = 1.4,\ \sigma_2 = 1.5,\ \sigma_3 = 1.6,\ \sigma_4 = 1.8$ have a significant decrease in φ while increasing ω.

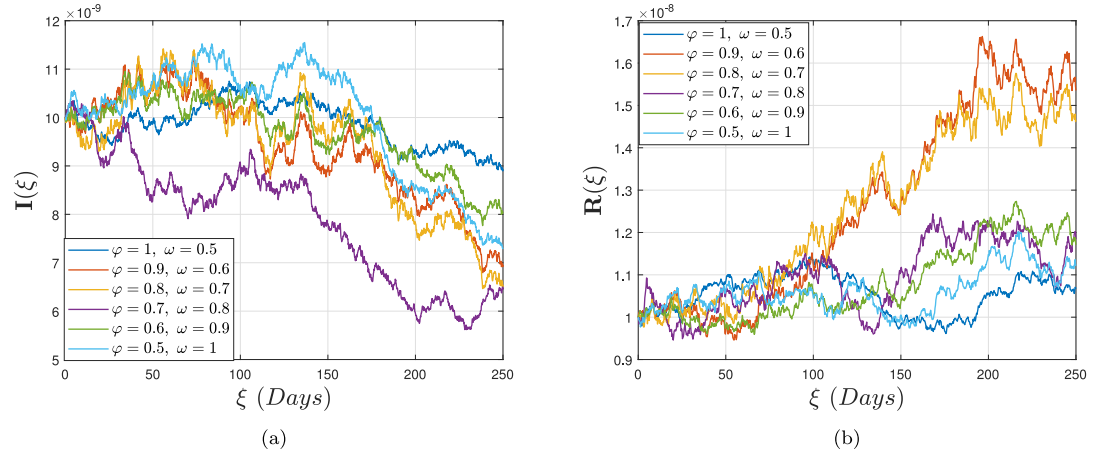

Fig. 9. Trajectories for the infected $\mathbf{I}(\xi)$ and restored $\mathbf{R}(\xi)$ when the white noise values $\sigma_1 = 1.4,\ \sigma_2 = 1.5,\ \sigma_3 = 1.6,\ \sigma_4 = 1.8$ have a significant decrease in φ while increasing ω.

using the F–F derivative scheme with a Mittag-Leffler kernel. As time passes, the increase in the number of infectious people becomes more visible; clearly, the curve $\mathbf{I}(\xi)$ is marginally greater for lower vaccination rates $\mathbf{q}$. Furthermore, the stochastic behaviour for increasing the fractal-dimension ω and decreasing the fractional-order φ yields intriguing results for reducing infection with low randomization densities. It is worthy to note that, in the randomized situation, the increase in the vaccination rate plays an important role in eradicating the infection.

Furthermore, we investigate how the restored efficiency ζ affects the growth of the estimated prevalence $\mathbf{I}(\xi)$ when the non-local and non-singular kernels are used. Figs. 10 and 11 show the test results obtained by varying the value of ζ while holding the other factors constant. The simulation findings demonstrate that as the level of the

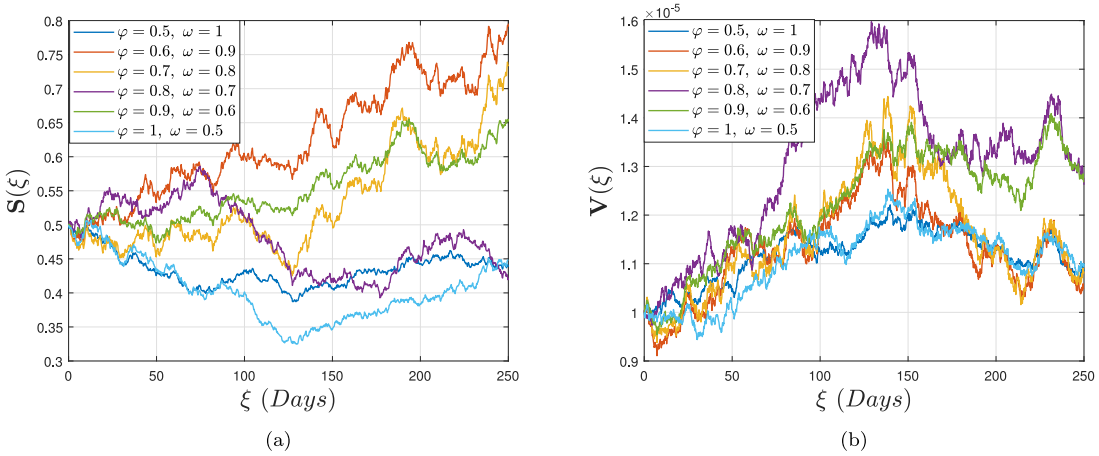

Fig. 10. Trajectories for the susceptible $\mathbf{S}(\xi)$ and vaccinated $\mathbf{V}(\xi)$ when the white noise values $\sigma_1 = 1.4,\ \sigma_2 = 1.5,\ \sigma_3 = 1.6,\ \sigma_4 = 1.8$ have a significant increase in φ while decreasing ω.

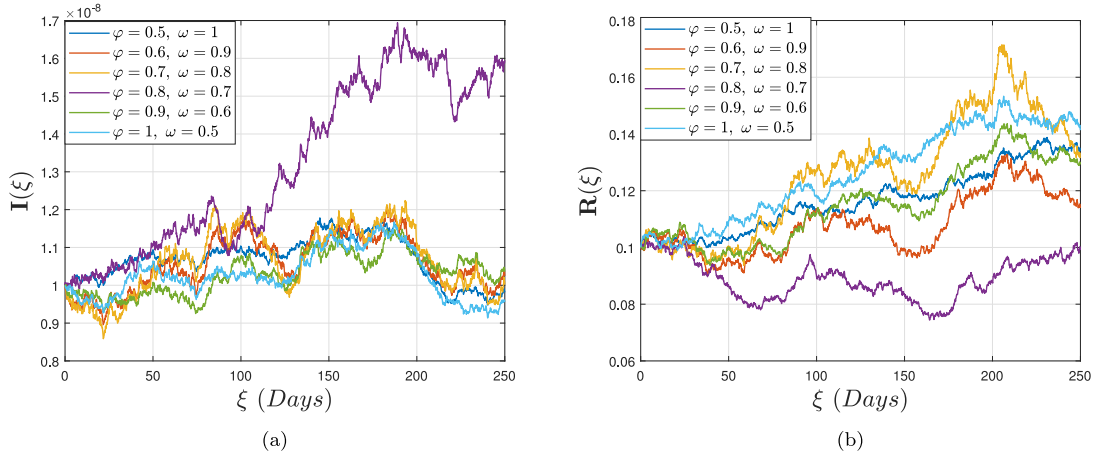

Fig. 11. Trajectories for the infected $\mathbf{I}(\xi)$ and restored $\mathbf{R}(\xi)$ when the white noise values $\sigma_1 = 1.4,\ \sigma_2 = 1.5,\ \sigma_3 = 1.6,\ \sigma_4 = 1.8$ have a significant increase in φ while decreasing ω.

recovery efficiency, ζ is increased, the incidence of tuberculosis patients drops. When φ and ω are increased in the above-mentioned Figs. 10 and 11, the decrease in affected patients is consistent in the findings presented by [14] but sporadic in the stochastic model. As a nutshell, we may deduce that increasing the value of the restoration factor ζ has a significant impact on eradicating the infection from the population.

Hence, numerical simulations are presented to verify the sufficient assumptions of the F–F derivative by incorporating the Brownian motions. In addition, analytical and experimental evaluations demonstrate that the noise effect's intensity is a key element in monitoring and inhibiting TB cell development in the vicinity of defencive effectors. Practitioners and therapeutic procedures benefit from the dynamical behaviour in the stochastic TB model. With the aid of environmental perturbations, therapeutic methods for TB victims can be changed for optimal performance throughout public interventions.

Conclusion

In this paper, we effectively offered a new evaluation of tuberculous using a novel modelling technique called fractal–fractional Atangana–Baleanu derivative via randomization. The fractal-dimension ω is used, and the fractional-order is φ. The problem is constructed adhering to Atangana–Baleanu's concept of F–F, and then certain supporting discoveries are provided. Then, for the formulation of the F–F model, we proposed an innovative numerical technique. Based on environmental unpredictability, the stochastic features are interconnected in the system as Gaussian white noise. In the midst of the infection, we generated certain necessary settings for permanence and elimination. When randomness is introduced into the deterministic SVIR system, the fundamental reproductive number is raised to a new threshold amount, $\mathbb{R}_0^{\mathbf{S}}$. It has been demonstrated that the disease will be eradicated if $\mathbb{R}_0^{\mathbf{S}} < 1$ is used. If $\mathbb{R}_0^{\mathbf{S}} > 1$, on the other hand, the sickness remains in the model, although still with distinct behaviours. However, when $\mathbb{R}_0^{\mathbf{S}} < 1$ and the level of white noise is high, the infection may be wiped off. In deterministic models, this does not arise. Graphical illustrations with the implementation of a stochastic SVIR model for newborn inoculation and F–F derivative in the Atangana–Baleanu sense give the capability to take into account environmental fluctuations that all influence the disease's transmission. The existence of a kernel (memory) in the modulation schemes allows for the regularity of eruptions. The researchers argue that the probabilistic SVIR model is an endeavour to comprehend TB infection features. When environmental noise (variability) and cross-immunity are addressed in TB disease systems, the framework is ideal for new insights into disease scenarios. In infectious diseases, combining white noise with fractional derivatives has a massive effect on the permanence and extermination of the outbreak, as well as enriching the model's kinetics. Our forthcoming research will concentrate on stochastic epidemic models incorporating Markovian switching, time delays and fractional calculus.

Declaration of competing interest

The authors declare that they have no known competing financial interests or personal relationships that could have appeared to influence the work reported in this paper.

Data availability

No data was used for the research described in the article.

Acknowledgement

All authors approved the version of the manuscript to be published.

References

[1] Bjune G. Tuberculosis in the 21st century: An emerging pandemic. Nor Epidemiol 2005;15:133–9.
[2] Brewer SJ, Hayman. To control and beyond: moving towards eliminating the global tuberculosis threat. J Epidemiol Commun Health 2004;58:822–5.
[3] Bhunu CP, Garira W, Mukandavire Z, Zimba M. Tuberculosis transmission model with chemoprophylaxis and treatment. Bull Math Biol 2008;70:1163–91.
[4] World Health Organization. Global tuberculosis control. 2019.
[5] Global tuberculosis report 2019. Geneva: World Health Organization; 2019, License, CC BY-NC-SA 3.0 IGO.
[6] Alene K, Viney K, Gray DJ, McBryde ES, Wagnew M, Clements ACA. Mapping tuberculosis treatment outcomes in Ethiopia. BMC Infect Dis 2019;19:474.
[7] FMOH. Guidelines for clinical and programmatic management of TB. In: TB/HIV and leprosy in Ethiopia. 6th edition. Addis Ababa, Ethiopia; 2016.
[8] CSIS. As Ethiopia moves toward tuberculosis elimination, success requires higher investment. 2016.
[9] Sintayehu S. Modeling the transmission of drug resistant tuberculosis in Ethiopia [Master Thesis], Addis Ababa, Ethiopia: Addis Ababa University; 2013.
[10] Moghadas SM, Gumel AB. Analysis of a model for transmission dynamics of TB. Can Appl Math Q 2002;10:411–28.
[11] World Health Organization. Global tuberculosis report. Switzerland: World Health Organization Press; 2014.
[12] Colditz CS, Berkey F, Mosteller TF, Brower ME, Wilson E, Burdick HV, et al. The efficacy of BCG vaccination of newborns and infants in the prevention of TB. 1995, Meta-analyses of the published literature.
[13] Corly. Differences between a baby, newborns, infant and toddler. 2020, January.
[14] Tilahun GT, Belachew MT, Gebreselassie Z. Stochastic model of tuberculosis with vaccination of newborns. Adv Differ Equ 2020;2020:658. http://dx.doi.org/10.1186/s13662-020-03122-w.
[15] Witbooi PJ, Muller GE, Van Schalkwyk GJ. Vaccination control in a stochastic SVIR epidemic model. Comput Math Methods Med 2015;9.
[16] Zwerling A, Shrestha S, Dowdy DW. Mathematical modeling and tuberculosis. In: Advances in diagnostics and novel therapies. 2015.
[17] Mengistu AK, Witbooi PJ. Modeling the effects of vaccination and treatment on tuberculosis transmission dynamics. J Appl Math 2019;9.
[18] Side S, Utami AM, Sukarna, Pratama MI. Numerical solution of SIR model for transmission of tuberculosis by Runge–Kutta method. J Phys 2018.
[19] Podlubny I. Fractional differential equations. San Diego: Academic Press; 1999.
[20] Caputo M, Fabrizio M. A new definition of fractional derivative without singular kernel. Prog Fract Differ Appl 2015;2:73–85.
[21] Atangana A, Baleanu D. New fractional derivatives with non-local and non-singular kernel theory and application to heat transfer model. Therm Sci 2016;20:763–9.
[22] Atangana A. Fractal-fractional differentiation and integration: Connecting fractal calculus and fractional calculus to predict complex system. Chaos Solitons Fractals 2017;396:102.
[23] Atangana A, Jain S. A new numerical approximation of the fractal ordinary differential equation. Eur Phys J Plus 2018;133:37.
[24] Rashid S, Ashraf R, Jarad F. Strong interaction of jafari decomposition method with nonlinear fractional-order partial differential equations arising in plasma via the singular and nonsingular kernels. AIMS Math 2022;7(5). http://dx.doi.org/10.3934/math.2022444.
[25] Rashid S, Jarad F, Ahmad AG, Abualnaja KM. New numerical dynamics of the heroin epidemic model using a fractional derivative with Mittag-Leffler kernel and consequences for control mechanisms. Results Phys 2022;35. http://dx.doi.org/10.1016/j.rinp.2022.105304.
[26] Bellman R, Cooke KL. Differential-difference equations. Academic Press; 1963.
[27] Arnold L. Stochastic differential equations: theory and applications. Wiley; 1974.
[28] Friedman A. Stochastic differential equations and applications, vol. 1. Academic Press; 1975.
[29] Luo ACJ, Afraimovich V. Long-range interactions, stochasticity and fractional dynamics: dedicated to George M. Zaslavsky. Springer; 2010.
[30] Ladde AG, Ladde GS. Dynamic processes under random environment. Bull Marathwada Math Soc 2007;8:96–123.
[31] Elliott RJ. Stochastic calculus and applications. New York: SpringerVerlag; 1982.
[32] Ladde GS, Wu L. Stochastic modeling and statistical analysis on the stock price processes. Nonlinear Anal Theory Meth 2009;71:1203–8.
[33] Ladde GS, Wu L. Development of nonlinear stochastic models by using stock price data and basic statistics. Neural Parallel Sci Comput 2010;18:269–82.
[34] Atangana A, Araz SI. Modeling and forecasting the spread of COVID-19 with stochastic and deterministic approaches: Africa and Europe. Adv Differ Eqs 2021;2021:1–107.
[35] Alkahtani BST, Koca I. Fractional stochastic SIR model. Results Phys 2021;24:104124.
[36] B, Alkahtani ST, Alzaid SS. Stochastic mathematical model of Chikungunya spread with the global derivative. Results Phys 2021;20:103680.
[37] Mbokoma M, Oukouomi Noutchie SC. Mathematical analysis of a stochastic tuberculosis model. J Anal Appl 2017;15:21–50.
[38] Shen J-M, Yang Z-H, Qian W-M, Zhang W, Chu Y-M. Sharp rational bounds for the gamma function. Math Inequal Appl 2020;23:843–53.
[39] Diekmann O, Heesterbeek JAP, Roberts MG. The construction of next-generation matrices for compartmental epidemic models. J R Soc Interface 2010;7:873–85.
[40] Baldi P, Mazliak L, Priouret P, Pierre. Martingales and markov chains. Chapman and Hall; 1991.